

Sphere free energy of scalar field theories with cubic interactions

Simone Giombi,¹ Elizabeth Himwich,^{2,3} Andrei Katsevich,¹ Igor Klebanov,^{1,2} and Zimo Sun^{1,3}

¹ *Joseph Henry Laboratories, Princeton University, Princeton, NJ 08544, USA*

² *Princeton Center for Theoretical Science, Princeton University, Princeton, NJ 08544, USA*

³ *Princeton Gravity Initiative, Princeton University, Princeton, NJ 08544, USA*

Abstract

The dimensional continuation approach to calculating the free energy of d -dimensional Euclidean CFT on the round sphere S^d has been used to develop its $4 - \epsilon$ expansion for a number of well-known non-supersymmetric theories, such as the $O(N)$ model. The resulting estimate of the sphere free energy F in the 3D Ising model has turned out to be in good agreement with the numerical value obtained using the fuzzy sphere regularization. In this paper, we develop the $6 - \epsilon$ expansions for CFTs on S^d described by scalar field theory with cubic interactions and use their resummations to estimate the values of F . In particular, we study the theories with purely imaginary coupling constants, which describe non-unitary universality classes arising when certain conformal minimal models are continued above two dimensions. The Yang-Lee model $M(2, 5)$ is described by a field theory with one scalar field, while the D -series $M(3, 8)$ model is described by two scalar fields. We also study the $OSp(1|2)$ symmetric cubic theory of one commuting and two anti-commuting scalar fields, which appears to describe the critical behavior of random spanning forests. In the course of our work, we revisit the calculations of beta functions of marginal operators containing the curvature. We also use another method for approximating F , which relies on perturbation theory around the bilocal action near the long-range/short-range crossover. The numerical values it gives for F tend to be in good agreement with other available methods.

Contents

1	Introduction and summary	3
2	Cubic scalar $O(N)$ theory	5
2.1	Flat-space warmup	5
2.2	Renormalization on the sphere	8
2.2.1	One-point function	10
2.2.2	Two-point function	12
2.2.3	Summary of beta functions for curvature couplings	13
3	Sphere free energy	13
4	Free energy in long-range approach	15
4.1	Setup	15
4.2	Quartic $O(N)$ model	17
4.3	Cubic $O(N)$ model	18
5	Numerical results for the sphere free energy	19
5.1	Quartic models	19
5.2	Cubic Lee-Yang model ($N = 0$)	22
5.3	$OSp(1 2)$ model (cubic $N = -2$)	23
5.4	Cubic $N = 1$ model	25
A	Flat space renormalization	27
B	Integral conventions on the sphere	28
C	Details of free energy calculations	29
C.1	Analytic calculation of $G_6^{(3)}$	31
D	Comparison of cubic $N = 0$ curvature couplings to previous literature	32
E	Details of long-range model calculations	33
E.1	Quartic model	33
E.2	Cubic model	34
	Bibliography	36

1 Introduction and summary

Studying d -dimensional Euclidean field theory on a round sphere S^d has a number of motivations, which range from infrared regularization of massless field theories [1] to Euclidean continuation of Quantum Field Theory in de Sitter space [2]. Our main motivation in this paper is related to defining measures of the number of degrees of freedom in Conformal Field Theory (CFT) [3–5]. A Euclidean CFT may be mapped from flat space \mathbb{R}^d to S^d of radius R using a Weyl transformation. Then the Euclidean path integral Z_{S^d} is regulated in the infrared, and the sphere free energy $F_{S^d} = -\log Z_{S^d}$ provides a very useful measure of the number of degrees of freedom. For even d , F_{S^d} grows as $\log R$ due to the Weyl anomaly. For example, for $d = 2$, $F_{S^2} = -\frac{c}{3} \log R + \dots$, where c is the Weyl anomaly coefficient, which is the central charge of the Virasoro algebra. It provides an important measure of the number of degrees of freedom in a CFT, and for unitary theories it decreases along Renormalization Group (RG) flow; this is the celebrated c theorem [6]. Analogously, in $d = 4$, $F_{S^4} = a \log R + \dots$, where a is a Weyl anomaly coefficient; it satisfies the a theorem [3, 7, 8].

For odd-dimensional CFTs, there is no Weyl anomaly, so that the sphere free energy is independent of R . It is a non-local observable, a pure number characterizing the CFT. The sphere free energy satisfies an RG inequality, $F_{\text{UV}} > F_{\text{IR}}$, called the F -theorem [4, 5, 9]. Just like the c and a theorems, it is generally applicable only to unitary theories. A physical interpretation of F is that it equals the long-range part of the Quantum Entanglement Entropy across a $d - 2$ dimensional sphere [10]. This connection with the Entanglement Entropy has enabled a proof of the F -theorem in the $d = 3$ case [11].

The calculation of the sphere free energy F in some 3D CFTs with extended supersymmetry may be reduced to finite dimensional integrals using the methods of localization [12]. For the well-known non-supersymmetric CFTs, such as the $O(N)$ vector model, the Gross-Neveu-Yukawa theory, and conformal QED, one instead has to resort to approximate methods for calculating F . They include the $1/N$ expansion [5, 13, 14] and dimensional continuation of the smooth quantity $\tilde{F} = -\sin\left(\frac{\pi d}{2}\right) F$ [15–18]. More recently, a novel numerical method for studying 3D CFTs was introduced [19], and it is attracting considerable interest (see also [20, 21] for applications of this approach to boundary CFTs). This method relies on mapping the spectrum of operator dimensions to the energy spectrum on the spatial 2-sphere supplied with a “fuzzy sphere” regulator. For the case of the 3D Ising model, the fuzzy sphere approach has produced excellent agreement with other calculations of the spectrum of scaling dimensions. This method can also be applied to the calculation of F , since it may be defined as the Entanglement Entropy across the equator of the spatial sphere. The numerical evaluation of this quantity for the 3D Ising model [22] produced excellent agreement with the earlier result found via dimensional continuation [15, 16]. This success motivates us to revisit the dimensional continuation approach to calculating F and extend it to

additional conformal models that are non-unitary.

We will also use another method for approximating F , which we call the Long Range Approach (LRA). It consists of beginning with the free long-range bilocal action (4.2), adjusting its parameter s to match the field dimension in the usual short-range CFT, and subsequently including the interaction corrections perturbatively. We will find that the LRA tends to agree well with the dimensional continuation approach, and in some cases may work even better.

One of the topics of this paper is the sphere free energy for theories of $N + 1$ scalar fields $\phi^i, i = 1, \dots, N$ and σ with cubic interactions $\frac{1}{2}g_1\sigma\phi^i\phi^i + \frac{1}{6}g_2\sigma^3$. When N is sufficiently large, these theories possess real perturbative fixed points that describe continuation of the $O(N)$ model above 4 dimensions [23]. The $6 - \epsilon$ expansion of this theory has been studied at higher orders [24–26], and the $1/N$ expansion of the sphere free energy was presented in [14]. In this paper, we instead focus on the fixed points with purely imaginary coupling constants, which are present for $N \leq 1$ [24].¹ The earliest and best-known example is $N = 0$; it is the theory of one scalar field with the $i\sigma^3$ interaction, which describes the Yang-Lee universality class [31]. When continued from $6 - \epsilon$ to 2 dimensions, it becomes equivalent to the $M(2, 5)$ non-unitary conformal minimal model [32] with central charge $-\frac{22}{5}$. A similar theory with $N = 1$ [24], which has been receiving some attention recently [33–36], describes the universality class of the D -series $M(3, 8)$ non-unitary minimal model; its central charge is $c(3, 8) = -\frac{21}{4}$. We will also consider the formal continuation to $N = -2$, which is described by one commuting and two anti-commuting scalar fields (a pair of symplectic fermions). Such a theory has an $OSp(1|2)$ invariant fixed point in $6 - \epsilon$ dimensions [37, 38]. It is equivalent to the formal $q \rightarrow 0$ limit of the critical q -state Potts model, which describes random spanning forests. This non-unitary statistical model, which is critical in $2 < d < 6$ dimensions, has been studied using various mathematical and numerical methods [39–41].

Using dimensional continuation methods similar to those in [14–16], we will study the sphere free energies of the Yang-Lee, $M(3, 8)$, and $OSp(1|2)$ universality classes. The necessary Feynman diagrams can be evaluated using Mellin-Barnes integrals with the Mathematica packages `MB.m` [42–45] as described in Appendix B of [16], to which we refer readers for details. The $6 - \epsilon$ expansion of \tilde{F} is affected by the existence of nearly marginal curvature terms \mathcal{R}^3 , $\mathcal{R}^2\sigma$, $\mathcal{R}\sigma^2$ and $\mathcal{R}\phi^i\phi^i$. We calculate the beta functions for these terms, and find results differing from some of the earlier literature. We find that, with the exception of \mathcal{R}^3 , the curvature terms do not affect the expansion of \tilde{F} up to order ϵ^3 .

This paper is organized as follows. In Section 2, we consider renormalization of the $O(N)$ cubic model. We begin with a flat-space warmup/review in Section 2.1 before turning to the renormalization of curvature couplings in Section 2.2. In Section 3, we discuss the sphere free energy and its renormalization in dimensional regularization. In Section 4 we consider a different

¹For scalar field theories with $O(N)^3$ symmetry [27, 28], there are large N melonic fixed points with imaginary tetrahedral coupling constant [29]. The sphere free energy in melonic theories was studied in [29, 30].

calculation of the sphere free energy in long-range models, with both quartic (Section 4.2) and cubic (Section 4.3) interactions. In Section 5 we discuss numerical results for the free energy, including its Padé approximant for cubic $N = 0, 1, -2$ models in dimensional regularization and a comparison with results from long-range models. Appendix A reviews renormalization of the $O(N)$ cubic model in flat space, Appendix B summarizes our conventions for integrals on the sphere, Appendix C includes details of the free energy calculation in dimensional regularization and an example integral evaluation, Appendix D compares our results for $N = 0$ with previous literature, and Appendix E includes details of the free energy calculations using the Long Range Approach.

2 Cubic scalar $O(N)$ theory

In this section, we consider the renormalization of the $O(N)$ cubic model on a sphere in $d = 6 - \epsilon$ dimensions. We first introduce the model and review its renormalization in flat space, and then discuss the renormalization of curvature counterterms.

2.1 Flat-space warmup

The flat-space cubic $O(N)$ theory in $d = 6 - \epsilon$ dimensions was introduced in [23], and its renormalization was further studied in [24, 25, 37, 46–50].² The bare action for the $O(N)$ -symmetric model of $N + 1$ scalar fields in flat space is

$$S = \int d^d x \left(\frac{1}{2} (\partial_\mu \phi_0^i)^2 + \frac{1}{2} (\partial_\mu \sigma_0)^2 + \frac{1}{2} g_{1,0} \sigma_0 \phi_0^i \phi_0^i + \frac{1}{3!} g_{2,0} \sigma_0^3 \right), \quad (2.1)$$

where σ_0 and ϕ_0^i , $i = 1, \dots, N$ are bare scalar fields and $g_{1,0}$, $g_{2,0}$ are bare couplings with classical scaling dimension $\epsilon/2$ in $d = 6 - \epsilon$. To renormalize the theory, one introduces renormalized fields and coupling constants

$$\phi_0^i = Z_\phi^{\frac{1}{2}} \phi^i, \quad \sigma_0 = Z_\sigma^{\frac{1}{2}} \sigma, \quad g_{1,0} = \mu^{\frac{\epsilon}{2}} Z_\phi^{-1} Z_\sigma^{-\frac{1}{2}} Z_{g_1} g_1, \quad g_{2,0} = \mu^{\frac{\epsilon}{2}} Z_\sigma^{-\frac{3}{2}} Z_{g_2} g_2, \quad (2.2)$$

where μ is an auxiliary scale and

$$Z_\phi = 1 + \delta_\phi, \quad Z_\sigma = 1 + \delta_\sigma, \quad Z_{g_1} = 1 + \frac{\delta_{g_1}}{g_1}, \quad Z_{g_2} = 1 + \frac{\delta_{g_2}}{g_2}. \quad (2.3)$$

In this section, we use dimensional regularization [62] in $d = 6 - \epsilon$ and the minimal subtraction renormalization scheme [63]. A summary of previous results for flat-space renormalization are collected for reference in Appendix A.

²Early studies of the $N = 0$ case in $d = 6 - \epsilon$ were performed in [31, 51–54]. Studies of this model have also been performed using the functional renormalization group [55–59] and conformal bootstrap [60, 61].

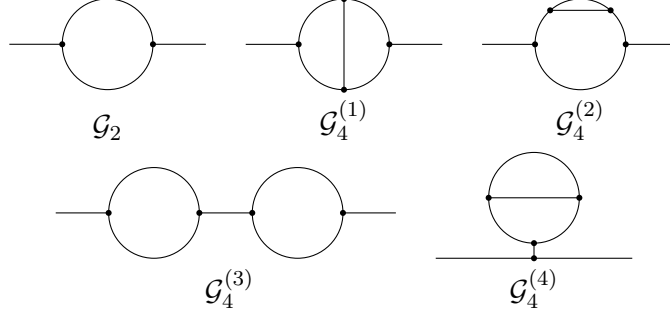


Figure 2.1: One and two-loop corrections to the propagator to order $\mathcal{O}(g_1^{n_1} g_2^{n_2})$ with $n_1 + n_2 = 4$.

As a warmup example of our method, it is instructive to review the scalar two-point function renormalization. While the momentum-space representation of Feynman diagrams is very helpful in flat space, there is no simple analog on the sphere, where we instead work in position space. When moving from momentum space to position space, it is important to keep track of reducible diagrams. For instance, consider the momentum-space two-point function of scalar fields $\langle \varphi_0(p) \varphi_0(-p) \rangle$, where φ_0 is either σ_0 or ϕ_0^i , and $\varphi_0 = Z_\varphi^{1/2} \varphi$. Defining $\Sigma(p^2)$ as the sum of all one-particle-irreducible insertions into the propagator, the full two-point function in momentum-space is given by the geometric series

$$\langle \varphi_0(p) \varphi_0(-p) \rangle = \frac{1}{p^2} + \frac{1}{p^2} \Sigma(p^2) \frac{1}{p^2} + \frac{1}{p^2} \Sigma(p^2) \frac{1}{p^2} \Sigma(p^2) \frac{1}{p^2} + \dots = \frac{1}{p^2 - \Sigma(p^2)}. \quad (2.4)$$

In turn, $\Sigma(p^2)$ can be expanded as a sum over k -loop diagrams denoted $\Sigma_k(p^2)$, which each have $2k$ powers of the cubic coupling g_0 :

$$\Sigma(p^2) = g_0^2 \Sigma_1(p^2) + g_0^4 \Sigma_2(p^2) + \dots. \quad (2.5)$$

One often discusses momentum-space renormalization conditions on the one-particle-irreducible diagrams $\Sigma(p^2)$. However, it is important to remember that when renormalizing the two-point function by requiring that $Z_\varphi^{-1} \langle \varphi_0(p) \varphi_0(-p) \rangle$ is finite order-by-order in g^2 , reducible diagrams will appear in the expansion (2.4). For instance, at $\mathcal{O}(g^4)$, the irreducible diagrams $\frac{1}{p^2} \Sigma_2(p^2) \frac{1}{p^2}$ as well as the reducible diagrams $\frac{1}{p^2} \Sigma_1(p^2) \frac{1}{p^2} \Sigma_1(p^2) \frac{1}{p^2}$ will contribute. The same diagrams appear in the position-space calculation, which is equivalent.

In the cubic scalar $O(N)$ theory, the flat position-space two-point functions to order $\mathcal{O}(g_1^{n_1} g_2^{n_2})$

with $n_1 + n_2 = 4$ are (see Figure 2.1)

$$\begin{aligned} \langle \sigma_0(x)\sigma_0(y) \rangle = \mathbb{G}_d(x, y) & \left(1 + \frac{N g_{1,0}^2 + g_{2,0}^2}{2} \mathcal{G}_2 + \frac{N g_{1,0}^4 + 2N g_{1,0}^3 g_{2,0} + g_{2,0}^4}{2} \mathcal{G}_4^{(1)} \right. \\ & + \frac{2N g_{1,0}^4 + N g_{1,0}^2 g_{2,0}^2 + g_{2,0}^4}{2} \mathcal{G}_4^{(2)} + \frac{N^2 g_{1,0}^4 + 2N g_{1,0}^2 g_{2,0}^2 + g_{2,0}^4}{4} \mathcal{G}_4^{(3)} \\ & \left. + \frac{2N g_{1,0}^3 g_{2,0} + N g_{1,0}^2 g_{2,0}^2 + g_{2,0}^4}{4} \mathcal{G}_4^{(4)} + \dots \right), \end{aligned} \quad (2.6)$$

$$\begin{aligned} \langle \phi_0^i(x)\phi_0^j(y) \rangle = \delta^{ij} \mathbb{G}_d(x, y) & \left(1 + g_{1,0}^2 \mathcal{G}_2 + (g_{1,0}^4 + g_{1,0}^3 g_{2,0}) \mathcal{G}_4^{(1)} + \frac{(N+2)g_{1,0}^4 + g_{1,0}^2 g_{2,0}^2}{2} \mathcal{G}_4^{(2)} \right. \\ & \left. + g_{1,0}^4 \mathcal{G}_4^{(3)} + \frac{2N g_{1,0}^4 + N g_{1,0}^3 g_{2,0} + g_{1,0} g_{2,0}^3}{4} \mathcal{G}_4^{(4)} + \dots \right), \end{aligned} \quad (2.7)$$

where we have pulled out an overall factor of the massless propagator $\mathbb{G}_d(x, y)$ defined in (B.5), and the dots denote $\mathcal{O}(g_1^{n_1} g_2^{n_2})$ with $n_1 + n_2 = 6$. Using Mellin-Barnes integrals [42–45] to evaluate the diagrams, we find

$$\begin{aligned} \mathcal{G}_2 &= -\frac{1}{3(4\pi)^3} \left(\frac{1}{\epsilon} + \frac{5/3 + \gamma_E + \log(\pi) + \log|x-y|^2}{2} + \mathcal{O}(\epsilon) \right), \\ \mathcal{G}_4^{(k)} &= -\frac{1}{3(4\pi)^6} \begin{cases} \frac{1}{\epsilon^2} + \frac{2+\gamma_E+\log(\pi)+\log|x-y|^2}{\epsilon} + \mathcal{O}(1), & k=1, \\ -\frac{1}{6} \left(\frac{1}{\epsilon^2} + \frac{31/12+\gamma_E+\log(\pi)+\log|x-y|^2}{\epsilon} \right) + \mathcal{O}(1), & k=2, \\ -\frac{1}{3} \left(\frac{1}{\epsilon^2} + \frac{5/3+\gamma_E+\log(\pi)+\log|x-y|^2}{\epsilon} \right) + \mathcal{O}(1), & k=3, \\ \mathcal{O}(1), & k=4, \end{cases} \end{aligned} \quad (2.8)$$

where γ_E is the Euler-Mascheroni constant. When the two-point function is expressed in terms of the renormalized couplings via (2.2), additional factors of $\log \mu$ will make the argument of the sub-leading logarithm dimensionless. Combining all the diagrams and requiring that $Z_\phi^{-1} \langle \phi_0^i(x)\phi_0^j(y) \rangle$ and $Z_\sigma^{-1} \langle \sigma_0(x)\sigma_0(y) \rangle$ are finite, we recover the wavefunction renormalization (A.5) and (A.6). Note that the reducible diagram $\mathcal{G}_4^{(3)}$ in Fig. 2.1 must be included to obtain the correct result.

An additional consideration in the flat-space theory is that the operators $\phi^i \phi^i$ and σ^2 mix under renormalization. The one-loop anomalous dimension matrix γ_{ab} , $1 \leq a, b \leq 2$ was computed in [23]. Denote its eigenvalues by γ_\pm ($\gamma_+ > \gamma_-$ in our convention) and the corresponding eigenoperators by \mathbb{O}^\pm . At the fixed point, to the leading order in the ϵ -expansion [23],

$$\Delta_+ = d - 2 + \gamma_+ \frac{g_i^*}{\mu} 2 + \Delta_\sigma, \quad (2.9)$$

where $\Delta_\sigma = \frac{d-2}{2} + \gamma_\sigma$ and $\gamma_\sigma \equiv -\frac{1}{2} \mu \frac{\partial}{\partial \mu} \log Z_\sigma$. The operator \mathbb{O}^+ is thus indeed a descendant of σ , as suggested by its equation of motion. To obtain the equality (2.9) at the fixed point, which

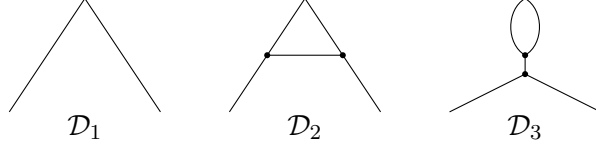


Figure 2.2: One-loop renormalization of σ_0^2 . The diagrams represent the three-point function $\langle \sigma^2(p+q)\sigma(p)\sigma(q) \rangle$. Diagrams with external leg corrections are omitted.

is the expected relation for a conformal descendant, it is essential to include reducible diagrams in the renormalization of $\phi^i\phi^i$ and σ^2 .

As an explicit example, for $N = 0$ (with $g_1 = 0$ and $g \equiv g_2$), the primary \mathbb{O}^- drops out and \mathbb{O}^+ is simply σ^2 . The one-loop result is taken from [23]:

$$\Delta_{\sigma^2} = d - 2 + \gamma_{\sigma^2}, \quad \gamma_{\sigma^2} = -\frac{2g^2}{3(4\pi)^3}. \quad (2.10)$$

At the fixed point $\frac{g^{*2}}{(4\pi)^3} = -\frac{2}{3}\epsilon$ from (A.11), we check that to order ϵ ,

$$\Delta_{\sigma^2} \stackrel{g^*}{=} 2 + \Delta_{\sigma}, \quad (2.11)$$

where from (A.4) we have

$$\Delta_{\sigma} = \frac{4 - \epsilon}{2} + \gamma_{\sigma}, \quad \gamma_{\sigma} = \frac{g^2}{12(4\pi)^3}, \quad (2.12)$$

which is consistent with the fact that σ^2 is a descendant of σ , i.e. $\partial^2\sigma \sim \sigma^2$. In order to obtain this descendant relation $\Delta_{\sigma^2} = 2 + \Delta_{\sigma}$, it is crucial to include the reducible diagram \mathcal{D}_3 (see Figure 2.2) in the renormalization of σ_0^2 . Dropping \mathcal{D}_3 and only including the irreducible diagrams gives the leading anomalous dimension (see e.g. [26, 51]) $\gamma_{\sigma^2}^{\text{irred.}} = -\frac{5g^2}{6(4\pi)^3}$. This leads to the relation $2 + \Delta_{\sigma} \stackrel{g^*}{=} 4 - \gamma_{\sigma^2}^{\text{irred.}}$ (instead of what we expect to be the descendant relation) and to a shadow relation $\Delta_{\sigma} + \Delta_{\sigma^2}^{\text{irred.}, g^*} \stackrel{g^*}{=} d = 6 - \epsilon$.

2.2 Renormalization on the sphere

The generalization of the cubic scalar $O(N)$ model to the sphere $S^{6-\epsilon}$ was considered in [15] and [14], which respectively computed the leading and subleading terms in the ϵ -expansion of the sphere free energy. To renormalize the theory in curved space, one must consider all independent consistent curvature couplings that are nearly marginal in $d = 6 - \epsilon$, following [64–67]. On the sphere, we

thus have the following bare action for the $O(N)$ -symmetric cubic model of $N + 1$ scalar fields:

$$S = \int d^d x \sqrt{g} \left(\frac{1}{2} (\partial_\mu \phi_0^i)^2 + \frac{1}{2} (\partial_\mu \sigma_0)^2 + \frac{\xi}{2} \mathcal{R} (\phi_0^i \phi_0^i + \sigma_0^2) + \frac{1}{2} g_{1,0} \sigma_0 \phi_0^i \phi_0^i + \frac{1}{3!} g_{2,0} \sigma_0^3 + \frac{\eta_{1,0}}{2} \mathcal{R} \phi_0^i \phi_0^i + \frac{\eta_{2,0}}{2} \mathcal{R} \sigma_0^2 + \kappa_0 \mathcal{R}^2 \sigma_0 + b_0 \mathcal{R}^3 \right), \quad (2.13)$$

where \mathcal{R} is the Ricci scalar curvature, σ_0 and ϕ_0^i , $i = 1, \dots, N$ are bare conformally coupled scalar fields with $\xi = \frac{d-2}{4(d-1)}$, and $g_{1,0}$, $g_{2,0}$, $\eta_{1,0}$, $\eta_{2,0}$, κ_0 , and b_0 are bare couplings. Note that we have separated arbitrary couplings $\eta_{1,0}$ and $\eta_{2,0}$ from the conformal coupling term ξ , and that a linear term in ϕ_0^i is forbidden by $O(N)$ symmetry. In $d = 6 - \epsilon$ dimensions, κ has classical scaling dimension $-\epsilon/2$, η has dimension zero, and b has dimension $-\epsilon$. Our conventions for propagators and integrals on the sphere are collected in Appendix B.

Following the definitions (2.2) and (2.3) in flat space, on the sphere we introduce renormalized fields and coupling constants

$$\begin{aligned} \phi_0^i &= Z_\phi^{\frac{1}{2}} \phi^i, & \sigma_0 &= Z_\sigma^{\frac{1}{2}} \sigma, & g_{1,0} &= \mu^{\frac{\epsilon}{2}} Z_\phi^{-1} Z_\sigma^{-\frac{1}{2}} Z_{g_1} g_1, & g_{2,0} &= \mu^{\frac{\epsilon}{2}} Z_\sigma^{-\frac{3}{2}} Z_{g_2} g_2, \\ \eta_{1,0} &= Z_\phi^{-1} Z_{\eta_1} \eta_1, & \eta_{2,0} &= Z_\sigma^{-1} Z_{\eta_2} \eta_2, & \kappa_0 &= \mu^{-\frac{\epsilon}{2}} Z_\sigma^{-\frac{1}{2}} Z_\kappa \kappa, & b_0 &= \mu^{-\epsilon} Z_b b, \end{aligned} \quad (2.14)$$

where μ is an auxiliary scale and

$$\begin{aligned} Z_\phi &= 1 + \delta_\phi, & Z_\sigma &= 1 + \delta_\sigma, & Z_{g_1} &= 1 + \frac{\delta_{g_1}}{g_1}, & Z_{g_2} &= 1 + \frac{\delta_{g_2}}{g_2}, \\ Z_{\eta_1} &= 1 + \frac{\delta_{\eta_1}}{\eta_1}, & Z_{\eta_2} &= 1 + \frac{\delta_{\eta_2}}{\eta_2}, & Z_\kappa &= 1 + \frac{\delta_\kappa}{\kappa}, & Z_b &= 1 + \frac{\delta_b}{b}. \end{aligned} \quad (2.15)$$

The renormalization of g_1 and g_2 on the sphere is the same as in flat space, and was computed in [23–26] (see Appendix A for a summary). For the renormalization of the sphere free energy to order ϵ^2 in Section 3, we need the relation between the bare and renormalized g_1 and g_2 couplings to quartic order, which are shown in (A.9) and (A.10).

The next-to-leading term in the sphere free energy for large N was computed in [14], to which order the contribution of η_1 , η_2 , and κ was assumed to vanish. The renormalization of b was then determined by finiteness of the renormalized sphere free energy to sixth order in g_1 and g_2 , which was also assumed to be independent of η_1 , η_2 , and κ . Here, we determine the renormalization of η_1 , η_2 , and κ directly from finiteness of the renormalized one- and two-point functions of ϕ and σ . A priori, renormalization of the curvature couplings can depend on any of the marginal couplings involving ϕ or σ in the action. The curvature counterterms are expanded

$$\delta_{\eta_1, \eta_2} = \sum_{n=1}^{\infty} \frac{\delta_{\eta_1, \eta_2}^{(n)}}{\epsilon^n}, \quad \delta_\kappa = \sum_{n=1}^{\infty} \frac{\delta_\kappa^{(n)}}{\epsilon^n}, \quad \delta_b = \sum_{n=1}^{\infty} \frac{\delta_b^{(n)}}{\epsilon^n}. \quad (2.16)$$

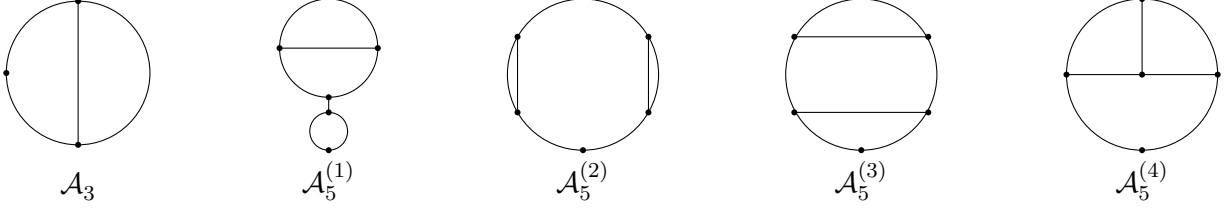


Figure 2.3: Diagrams up to order $\mathcal{O}(g_1^{n_1} g_2^{n_2})$ with $n_1 + n_2 = 5$ that contribute to the one-point function of σ . The external leg is amputated.

Using our results, we will see in Section 3 that the renormalized curvature couplings do not contribute to the renormalized free energy at the fixed point at order ϵ^2 , justifying the assumptions of [14].

2.2.1 One-point function

Here, we compute the one-point function $\langle \sigma_0 \rangle$ on the sphere and renormalize $\langle \sigma \rangle = Z_\sigma^{-\frac{1}{2}} \langle \sigma_0 \rangle$. Note that the one-point function is position-independent due to $SO(d+1)$ symmetry. First, we consider the contributions purely from g_1 and g_2 . At order $\mathcal{O}(g_1^{n_1} g_2^{n_2})$ with $n_1 + n_2 = 1$, the tadpole diagram vanishes in dimensional regularization. At order $\mathcal{O}(g_1^{n_1} g_2^{n_2})$ with $n_1 + n_2 = 3$, there is only one diagram, i.e. \mathcal{A}_3 in Figure 2.3. At order $\mathcal{O}(g_1^{n_1} g_2^{n_2})$ with $n_1 + n_2 = 5$, the $\mathcal{A}_5^{(a)}$ diagrams in Figure 2.3 contribute. Altogether, these diagrams yield

$$\langle \sigma_0 \rangle = - \left(a_3 \mathcal{A}_3 + a_{5,1} \mathcal{A}_5^{(1)} + a_{5,2} \mathcal{A}_5^{(2)} + a_{5,3} \mathcal{A}_5^{(3)} + a_{5,4} \mathcal{A}_5^{(4)} \right) \frac{C_d I_2(\frac{d-2}{2})}{\text{Vol}(S^d)} + \dots, \quad (2.17)$$

where the constants $\text{Vol}(S^d)$ and C_d are defined in (B.2) and (B.4), the integral I_2 is defined in (B.6), the factor $\frac{C_d I_2(\frac{d-2}{2})}{\text{Vol}(S^d)} = \int d^d y \Omega^d(y) G_d(x, y)$ comes from the external leg, the dots denote contributions from curvature counterterms (considered below) as well as $\mathcal{O}(g_1^{n_1} g_2^{n_2})$ with $n_1 + n_2 = 7$, and the combinatorial factors for each diagram are

$$a_3 = \frac{1}{4} \left(2N g_{1,0}^3 + N g_{1,0}^2 g_{2,0} + g_{2,0}^3 \right),$$

$$a_{5,k} = \begin{cases} \frac{1}{8} \left(2N^2 g_{1,0}^5 + N^2 g_{1,0}^4 g_{2,0} + 2N g_{1,0}^3 g_{2,0}^2 + 2N g_{1,0}^2 g_{2,0}^3 + g_{2,0}^5 \right), & k = 1, \\ \frac{1}{8} \left(4N g_{1,0}^5 + N^2 g_{1,0}^4 g_{2,0} + 2N g_{1,0}^2 g_{2,0}^3 + g_{2,0}^5 \right), & k = 2, \\ \frac{1}{4} \left(N(N+2) g_{1,0}^5 + 2N g_{1,0}^4 g_{2,0} + N g_{1,0}^3 g_{2,0}^2 + N g_{1,0}^2 g_{2,0}^3 + g_{2,0}^5 \right), & k = 3, \\ \frac{1}{4} \left(2N g_{1,0}^5 + 3N g_{1,0}^4 g_{2,0} + 2N g_{1,0}^3 g_{2,0}^2 + g_{2,0}^5 \right), & k = 4. \end{cases} \quad (2.18)$$



Figure 2.4: Leading contributions of curvature terms to the one-point function. The empty dot represents an insertion of κ and the cross represents an η vertex.

The evaluation of \mathcal{A}_3 is presented as an analytic example in Appendix C.1. We find

$$\mathcal{A}_3 = (2R)^{8-2d} C_d^4 e^{\gamma_E(d-6) + \frac{\pi^2}{24}(d-6)^2} \pi^d \left(-\frac{1}{8} - \frac{11\epsilon}{32} + \mathcal{O}(\epsilon^2) \right),$$

$$\mathcal{A}_5^{(k)} = (2R)^{14-3d} C_d^7 e^{2\gamma_E(d-6) + \frac{\pi^2}{24}(d-6)^2} \pi^{2d} \begin{cases} \frac{1}{24\epsilon} + \frac{25}{144} + \mathcal{O}(\epsilon), & k=1, \\ \frac{1}{12\epsilon} + \frac{193}{432} + \mathcal{O}(\epsilon), & k=2, \\ -\frac{1}{12\epsilon} - \frac{13}{48} + \mathcal{O}(\epsilon), & k=3, \\ -\frac{1}{4\epsilon} - \frac{73}{48} + \mathcal{O}(\epsilon), & k=4, \end{cases} \quad (2.19)$$

where R is the radius of the sphere.

To renormalize the one-point function we impose that $\langle \sigma \rangle = Z_\sigma^{-1/2} \langle \sigma_0 \rangle$ is finite. Using (2.17) and the flat-space renormalization of σ (A.6), we find that the pure g_1 and g_2 contributions are finite up to the $\mathcal{O}(g_1^{n_1} g_2^{n_2})$ with $n_1 + n_2 = 5$. This implies that such terms do not contribute to the renormalization of κ .

Next, we consider the following leading contributions from diagrams with curvature couplings shown in Figure 2.4:

$$\langle \sigma_0 \rangle \supset - \left(\kappa_0 \mathcal{R}^2 \mathcal{K}_0 - \frac{N g_{1,0} \eta_{1,0} + g_{2,0} \eta_{2,0}}{2} \mathcal{R} \mathcal{K}_1 \right) \frac{C_d I_2(\frac{d-2}{2})}{\text{Vol}(S^d)}, \quad (2.20)$$

where

$$\mathcal{K}_0 = 1, \quad \mathcal{K}_1 = \frac{C_d^2 I_2(d-2)}{\text{Vol}(S^d)} = -\frac{2}{(4\pi)^3 R^2 \epsilon} + \mathcal{O}(1). \quad (2.21)$$

Since Z_σ begins at $\mathcal{O}(g_1^{n_1} g_2^{n_2})$ with $n_1 + n_2 = 2$ (see (A.6)), these leading curvature contributions imply that for $\langle \sigma \rangle = Z_\sigma^{-1/2} \langle \sigma_0 \rangle$ to be finite, we must have

$$\delta_\kappa^{(1)} = -\frac{N \eta_1 g_1 + \eta_2 g_2}{30(4\pi)^3} + \dots, \quad (2.22)$$

where we used the value of \mathcal{R} in (B.3), the dots denote $\mathcal{O}(g_1^{n_1} g_2^{n_2})$ with $n_1 + n_2 = 7$ as well as curvature contributions beginning at $\mathcal{O}(\eta^2 g, \eta g^3, \kappa g^4)$. Note that we do not need to include mixing of σ with \mathcal{R} for renormalization at this order, though it can contribute at higher orders.

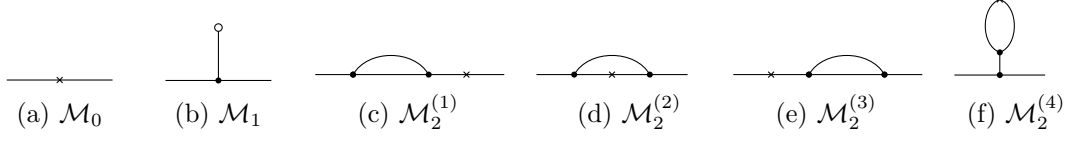


Figure 2.5: Leading contributions of curvature terms to the two-point function. The empty dot represents an insertion of κ and the cross represents an η vertex.

2.2.2 Two-point function

Next, we consider the renormalization of two-point functions of scalar fields. Again, we first consider the contribution of purely $g_{1,0}$ and $g_{2,0}$, and then consider contributions from the curvature vertices.

To generalize the calculations of Section 2.1 to the sphere, we make the choice of special points $x^2 = 1$ and $y = 0$. Computing these diagrams on the sphere, we find agreement with the flat space result (2.8) except with the flat space distance $|x - y|^2$ replaced by the corresponding distance $D(1, 0)^2 = \Omega(1)\Omega(0) = 2R^2$ on sphere. This agreement implies that we do not have a term $(g_1^{n_1} g_2^{n_2})\epsilon^{-1}$ with $n_1 + n_2 = 4$ in the η counterterm, which would renormalize the propagator.

Next, we consider the following leading contributions to the propagator from curvature couplings, where the diagrams are depicted in Figure 2.5:

$$\begin{aligned} \langle \sigma_0(x)\sigma_0(y) \rangle \supset G_d(x, y) & \left(-\eta_{2,0}\mathcal{R}\mathcal{M}_0 + g_{2,0}\kappa_0\mathcal{R}^2\mathcal{M}_1 - \frac{(Ng_{1,0}^2 + g_{2,0}^2)\eta_{2,0}}{2} (\mathcal{R}\mathcal{M}_2^{(1)} + \mathcal{R}\mathcal{M}_2^{(3)}) \right. \\ & \left. - (Ng_{1,0}^2\eta_{1,0} + g_{2,0}^2\eta_{2,0})\mathcal{R}\mathcal{M}_2^{(2)} - \frac{Ng_{1,0}g_{2,0}\eta_{1,0} + g_{2,0}^2\eta_{2,0}}{2}\mathcal{R}\mathcal{M}_2^{(4)} \right), \end{aligned} \quad (2.23)$$

$$\begin{aligned} \langle \phi_0^i(x)\phi_0^j(y) \rangle \supset \delta^{ij}G_d(x, y) & \left(-\eta_{1,0}\mathcal{R}\mathcal{M}_0 + g_{1,0}\kappa_0\mathcal{R}^2\mathcal{M}_1 - g_{1,0}^2\eta_{1,0} (\mathcal{R}\mathcal{M}_2^{(1)} + \mathcal{R}\mathcal{M}_2^{(3)}) \right. \\ & \left. - g_{1,0}^2(\eta_{1,0} + \eta_{2,0})\mathcal{R}\mathcal{M}_2^{(2)} - \frac{Ng_{1,0}^2\eta_{1,0} + g_{1,0}g_{2,0}\eta_{2,0}}{2}\mathcal{R}\mathcal{M}_2^{(4)} \right), \end{aligned} \quad (2.24)$$

where we have pulled out an overall factor of the sphere propagator $G_d(x, y)$. Evaluating the diagrams, again with the choice $x^2 = 1$ and $y = 0$, we find at the lowest order

$$\mathcal{M}_0 = R^2(1 - \log 2 + \mathcal{O}(\epsilon)), \quad \mathcal{M}_1 = \frac{C_d I_2(\frac{d-2}{2})}{\text{Vol}(S^d)} R^2(1 - \log 2 + \mathcal{O}(\epsilon)), \quad (2.25)$$

and for the diagrams quadratic in $g_{1,0}$ and $g_{2,0}$ we find

$$\mathcal{M}_2^{(1)} = \mathcal{M}_2^{(3)} = \mathcal{M}_2^{(4)} = R^2 \left(-\frac{1 - \log 2}{3(4\pi)^3 \epsilon} + \mathcal{O}(1) \right), \quad \mathcal{M}_2^{(2)} = R^2 \left(\frac{1 - \log 2}{(4\pi)^3 \epsilon} + \mathcal{O}(1) \right). \quad (2.26)$$

Now, imposing that $Z_\phi^{-1}\langle \phi_0^i(x)\phi_0^j(y) \rangle$ and $Z_\sigma^{-1}\langle \sigma_0(x)\sigma_0(y) \rangle$ are finite implies that the η_i counter-

erms in (2.16) are given by

$$\delta_{\eta_1}^{(1)} = -\frac{(\eta_1 + \eta_2)g_1^2}{(4\pi)^3\epsilon} + \dots, \quad (2.27)$$

$$\delta_{\eta_2}^{(1)} = -\frac{N\eta_1g_1^2 + \eta_2g_2^2}{(4\pi)^3\epsilon} + \dots, \quad (2.28)$$

where the dots denote $\mathcal{O}(g_1^{n_1}g_2^{n_2})$ with $n_1 + n_2 = 6$ as well as higher powers of curvature couplings beginning at $\mathcal{O}(\eta g^4)$.³

2.2.3 Summary of beta functions for curvature couplings

The bare couplings in (2.14) and (2.15) do not change with the arbitrary scale μ , which implies

$$\beta_\kappa = \frac{\epsilon}{2}\kappa + \frac{Ng_1^2 + g_2^2}{12(4\pi)^3}\kappa - \frac{N\eta_1g_1 + \eta_2g_2}{30(4\pi)^3} + \dots, \quad (2.29)$$

where the dots denote $\mathcal{O}(g_1^{n_1}g_2^{n_2})$ with $n_1 + n_2 = 7$ as well as curvature contributions beginning at $\mathcal{O}(\eta^2g, \eta g^3, \kappa g^4)$, and

$$\beta_{\eta_1} = -\frac{(2\eta_1 + 3\eta_2)g_1^2}{3(4\pi)^3} + \dots, \quad (2.30)$$

$$\beta_{\eta_2} = -\frac{6N\eta_1g_1^2 - N\eta_2g_1^2 + 5\eta_2g_2^2}{6(4\pi)^3} + \dots, \quad (2.31)$$

where the dots denote $\mathcal{O}(g_1^{n_1}g_2^{n_2})$ with $n_1 + n_2 = 6$ as well as higher powers of curvature couplings beginning at $\mathcal{O}(\eta g^4)$. This implies the following fixed points for the curvature couplings:

$$\eta_1^*, \eta_2^* = \mathcal{O}(\epsilon^2), \quad \kappa^* = \mathcal{O}(\epsilon^{\frac{3}{2}}). \quad (2.32)$$

In the next section, we will see that this behavior implies that the curvature couplings do not contribute to the $6 - \epsilon$ expansion of \tilde{F} to order ϵ^3 .

3 Sphere free energy

In this section, we review the computation of the renormalized sphere free energy $F = -\log Z$ and its generalization $\tilde{F} = -\sin\left(\frac{\pi d}{2}\right)F$ as defined in [15]. In odd dimensions, $\tilde{F} = (-1)^{\frac{d+1}{2}}F$. In even dimensions, $\tilde{F} = (-1)^{\frac{d}{2}}\frac{\pi}{2}a$, where a is the generalization of the Weyl anomaly coefficient [3, 8] in four dimensions, which is related by $c = -3a$ to the central charge studied by [6] in two dimensions.

³Note that the renormalization of η is independent of κ at leading order. We believe that this can be shown to all orders following arguments similar to those of [64, 65] demanding finiteness of the renormalized stress tensor. Also note that $\delta_{\eta_2}^{(1)}$ can be equivalently obtained from renormalizing the one-point function $\langle\sigma_0\rangle$.

For example, \tilde{F} for a conformally coupled free scalar reads on S^d reads

$$\tilde{F}_{\text{free}} = \frac{1}{\Gamma(1+d)} \int_0^1 du u \sin(\pi u) \Gamma\left(\frac{d}{2} + u\right) \Gamma\left(\frac{d}{2} - u\right), \quad (3.1)$$

where we have used (C.1).

The leading term in ϵ -expansion for the sphere free energy of (2.1) for general N was computed in [15] (also for the case $N = -2$ in [37]), and the next-to-leading term for large N was computed (without considering curvature vertices) in [14]. Here we include formulas of the next-to-leading term for general N , which we then specify to the cases $N = 0, -2, 1$, for which we also compute Padé approximants in Section 5. We define integrated connected sphere correlation functions

$$G_n = \int \prod_{i=1}^n d^d x_i \sqrt{g_{x_i}} \langle \varphi_0^3(x_1) \dots \varphi_0^3(x_n) \rangle_0^{\text{conn}}, \quad (3.2)$$

where $\varphi_0^3 \equiv 3g_{1,0}\sigma_0\phi_0^i\phi_0^i + g_{2,0}\sigma_0^3$. To compute the renormalized sphere free energy to order ϵ^2 , we need to consider the renormalization of contributions up to sixth order the couplings $g_{1,0}$ and $g_{2,0}$, for the following reason. The divergent part of these sixth-order terms has a pole in ϵ , which we remove by fixing the counterterms in b_0 (which also includes a contribution to remove the one-loop divergence of the conformally coupled scalar (C.1)). At the fixed point, b^* then will include a contribution of order ϵ^2 (a factor of ϵ^3 at the fixed point from the sixth order in g_1 and g_2 , multiplied by the ϵ^{-1} from the b_0 counterterms).

In addition to potentially finite contributions from the curvature couplings κ and η through order ϵ^2 at the fixed point, we must also consider the possibility that they lead to divergences at the same order as g^6 , which would contribute to renormalization of the free energy. Using the fixed points in the previous subsection (2.32), the three diagrams $\kappa^2 \circ\text{---}\circ$, $\eta g^2 \text{---}\text{---}\text{---}$, and $\kappa g^3 \text{---}\text{---}\text{---}$ can potentially contain divergences at the same order as g^6 and thus affect the renormalization of b_0 . However, the integrated correlation functions with these coefficients are all finite: the first diagram is proportional to $I_2(\frac{d-2}{2})$ (cf. (B.6)) and the rest are proportional to \mathcal{A}_3 (cf. (C.22)). Therefore, they do not contribute to the renormalized free energy at order ϵ^2 .

For the finite terms in the free energy at $\mathcal{O}(\epsilon^2)$ at the fixed point and renormalization at the next order, we can thus simply consider the same terms as in [14]:

$$F = (N+1)F_{\text{free}} - \frac{G_2}{2!(3!)^2} - \frac{G_4}{4!(3!)^4} - \frac{G_6}{6!(3!)^6} + b_0 \int d^d x \sqrt{g} \mathcal{R}^3, \quad (3.3)$$

where F_{free} is the sphere free energy for conformally coupled free scalar (C.1). The contribution from G_n and F_{free} for large N was computed in [14]. Here we write the result for general N . A review of previous results and more detailed explanation can be found in Appendix C.

Expressing the free energy in terms of the renormalized couplings at the fixed point

$$\beta_{g_1} = \beta_{g_2} = \beta_{\eta_1} = \beta_{\eta_2} = \beta_{\kappa} = \beta_b = 0 \quad (3.4)$$

using (C.19), and (2.32), we obtain $\tilde{F} = -\sin \frac{\pi d}{2} F$ at $d = 6 - \epsilon$:

$$\begin{aligned} \tilde{F} = & (N+1)\tilde{F}_{\text{free}} - \frac{(3Ng_1^{*2} + g_2^{*2})(30 + \epsilon(15(\gamma_E + \log(4\pi\mu^2 R^2)) + 56))\epsilon}{2^{10}3^45^2(4\pi)^2} \\ & + \frac{N(9(N-8)(\gamma_E + \log(4\pi\mu^2 R^2)) + 26N - 148)g_1^{*4}\epsilon}{2^{11}3^55(4\pi)^5} - \frac{N(3(\gamma_E + \log(4\pi\mu^2 R^2)) + 7)g_1^{*3}g_2^{*}\epsilon}{2^73^45(4\pi)^5} \\ & + \frac{N(26 + 9\gamma_E + 9\log(4\pi\mu^2 R^2))g_1^{*2}g_2^{*2}\epsilon}{2^{10}3^55(4\pi)^5} - \frac{(27(\gamma_E + \log(4\pi\mu^2 R^2)) + 58)g_2^{*4}\epsilon}{2^{11}3^55(4\pi)^5} \\ & + \frac{N(2(43N + 268)g_1^{*6} - 12(11N - 32)g_1^{*5}g_2^{*} + (11N + 950)g_1^{*4}g_2^{*2} + 84g_1^{*3}g_2^{*3} - 44g_1^{*2}g_2^{*4}) + 125g_2^{*6}}{2^{12}3^65(4\pi)^8} \\ & + \mathcal{O}(\epsilon^4). \end{aligned} \quad (3.5)$$

This result gives \tilde{F} at the fixed point for any N at $\mathcal{O}(\epsilon^3)$. Note we have now explicitly checked that curvature couplings κ and η_1, η_2 do not contribute.

4 Free energy in long-range approach

In this section, we study the renormalized sphere free energy in the scalar field theories using a d -dimensional model with a long-range kinetic term and a slightly relevant perturbation by an operator of dimension $d - \epsilon$ with $0 < \epsilon \ll 1$. We will first consider a quartic perturbation in Section 4.2 to compare this method with various results in the literature for the Wilson-Fisher fixed point. Long-range models with quartic interactions have a long history [68–70] and they have been studied recently in [71–76]. We will then consider a cubic perturbation in Section 4.3, which corresponds to the long-range versions of the Lee-Yang and related CFTs.

4.1 Setup

Here, we provide an introduction to our approach using the long-range model in the case of a single scalar field on S^d with an action of the general form

$$S = S_0 + \lambda_0 \int d^d x \sqrt{g_x} O_0(x), \quad (4.1)$$

where λ_0 is the UV bare coupling, O_0 is the bare operator of dimension $d - \varepsilon$, and S_0 is the action of a free scalar field with conformally invariant long-range kinetic term [68, 74, 77, 78]

$$S_0 = \frac{2^{s-1} \Gamma(\frac{d+s}{2})}{\pi^{\frac{d}{2}} \Gamma(-\frac{s}{2})} \int d^d x d^d y \sqrt{g_x} \sqrt{g_y} \frac{\varphi_0(x) \varphi_0(y)}{D(x, y)^{d+s}}, \quad (4.2)$$

where $D(x, y)$ is defined in (B.5), d is a fixed integer dimension, and s a parameter that we choose to depend on ε such that the perturbing (quartic or cubic) interaction for φ has consistent dimension $d - \varepsilon$. Note that with this normalization, the momentum-space propagator is simply $|p|^{-s}$. The free two-point function of φ_0 on the sphere in this model is

$$G_{d,s}(x, y) = \frac{C_{d,s}}{D(x, y)^{d-s}}, \quad C_{d,s} = \frac{\Gamma(\frac{d-s}{2})}{\pi^{\frac{d}{2}} 2^s \Gamma(\frac{s}{2})}. \quad (4.3)$$

In this long-range model, the scaling dimension of φ is fixed to be $\frac{d-s}{2}$ and it is not renormalized along the RG flow. Note that the free propagator for a usual scalar field with local action corresponds to $s = 2$. In the case of the $O(N)$ model with quartic interaction, it is expected that when s is near a certain value s_* , there is a crossover from the long-range to short-range fixed points [69, 70, 72, 73]. This value is such that the conformal dimension of φ is continuous at the crossover, namely $(d - s_*)/2 = \Delta_\varphi^{\text{SR}}$. In the long-range region $s < s_*$, φ has no anomalous dimension and its scaling dimension is fixed as $\frac{d-s}{2}$. At the short-range fixed point, φ has an anomalous dimension and its dimension is $\frac{1}{2}(d - 2 + 2\gamma_\varphi^{\text{SR}})$, which implies $s_* = 2 - 2\gamma_\varphi^{\text{SR}}$.

In long-range models of fixed integer dimension, we can define a generalized free energy

$$\tilde{F}^{\text{LR}} = \begin{cases} (-1)^{\frac{d+1}{2}} F^{\text{LR}}, & d \text{ odd,} \\ (-1)^{\frac{d}{2}} \frac{\pi}{2} a^{\text{LR}}, & d \text{ even,} \end{cases} \quad (4.4)$$

where $F^{\text{LR}} = -\log Z^{\text{LR}}$. In odd dimensions, F^{LR} is finite and independent of R for conformal theories and in even dimensions, a^{LR} is defined as the coefficient of the logarithmic term in $F^{\text{LR}} = a^{\text{LR}} \log R + \dots$, as in short-range theories. This normalization matches the normalization of \tilde{F} [15] in integer dimensions (the latter is defined for short-range models in dimensional regularization).

Fixing s in terms of ε by setting the UV dimension of the perturbing operator to be $\Delta_O = d - \varepsilon$, we can compute the generalized free energy in the long-range model

$$\tilde{F}^{\text{LR}} = \tilde{F}_{\text{free}}^{\text{LR}} + \delta \tilde{F}^{\text{LR}}, \quad (4.5)$$

where $\delta \tilde{F}^{\text{LR}}$ is the change in the generalized sphere free energy due to the interaction O_0 using perturbation theory in ε , and $\tilde{F}_{\text{free}}^{\text{LR}}$ is the generalized free energy for a free scalar in the long-range model (4.2), defined in odd and even dimensions in analogy with (4.4). Computing $\tilde{F}_{\text{free}}^{\text{LR}}$

is equivalent to evaluating the logarithm of the functional determinant of $D(x, y)^{-d-s}$, which is a conformal two-point function of scalar primary operators with scaling dimension $\Delta = \frac{d+s}{2}$ on S^d . Such functional determinants correspond to double trace deformations in large N CFT that holographically induce the transition from standard quantization to alternate quantization of the dual bulk operator in AdS [79]. Both CFT and AdS calculations [15, 79–83] give

$$\tilde{F}_{\text{free}}^{\text{LR}} = \frac{1}{\Gamma(1+d)} \int_0^{\frac{s}{2}} du u \sin(\pi u) \Gamma\left(\frac{d}{2} + u\right) \Gamma\left(\frac{d}{2} - u\right). \quad (4.6)$$

Taking $s = 2$ recovers (3.1), corresponding to the usual two-derivative kinetic term.

Generalizing what is believed to happen for the scaling dimensions, we will assume that at the long-range/short-range crossover $s = s_*$, the free energy of the long-range model smoothly goes to that of the short-range one.⁴ We will also assume that the same crossover picture discussed in the literature for the quartic models applies to the cubic models as well. Then, to compare with the results of the previous sections and previous literature, in Section 5 we evaluate \tilde{F}^{LR} at the short-range fixed point ε_* set by s_* . We denote the result $\tilde{F}^{\text{LRA}} \equiv \tilde{F}^{\text{LR}}|_{\varepsilon_*}$ for the short-range generalized free energy using the long-range approach.

4.2 Quartic $O(N)$ model

Our quartic $O(N)$ model with long-range kinetic term is given by

$$S = \frac{2^{s-1} \Gamma(\frac{d+s}{2})}{\pi^{\frac{d}{2}} \Gamma(-\frac{s}{2})} \int d^d x d^d y \sqrt{g_x} \sqrt{g_y} \frac{\phi_0^i(x) \phi_0^i(y)}{D(x, y)^{d+s}} + \frac{\lambda_0}{4} \int d^d x \sqrt{g_x} \left(\phi_0^i(x) \phi_0^i(x) \right)^2, \quad (4.7)$$

where $i = 1, \dots, N$ and we take $s = \frac{d+\varepsilon}{2}$ so that ϕ_0^i has dimension $\frac{d-\varepsilon}{4}$ and $(\phi_0^i \phi_0^i)^2$ is a nearly marginal operator of dimension $d - \varepsilon$. Define the renormalized coupling λ by

$$\lambda_0 = \mu^\varepsilon Z_\lambda \lambda, \quad Z_\lambda = 1 + \frac{\delta\lambda}{\lambda}. \quad (4.8)$$

Note that there is no wavefunction renormalization of ϕ^i in the long-range model. The beta function for λ was computed in [74] to order λ^3 :

$$\beta(\lambda) = -\varepsilon \lambda + \frac{2(N+8)}{(4\pi)^{\frac{d}{2}} \Gamma(\frac{d}{2})} \lambda^2 + \frac{8(5N+22)}{(4\pi)^d \Gamma(\frac{d}{2})^2} \left(\gamma_E + 2\psi\left(\frac{d}{4}\right) - \psi\left(\frac{d}{2}\right) \right) \lambda^3 + \mathcal{O}(\lambda^4), \quad (4.9)$$

⁴In [72], it was proposed that at the crossover the long-range model goes over to the short-range model plus a decoupled non-local scalar field χ with $\Delta_\chi = (d+s)/2$, rather than to the short-range model alone. If that proposal is understood to hold as a statement about the partition functions of the models, then it would imply that $F_{s=s_*}^{\text{LR}} = F^{\text{SR}} + F_\chi$. This appears to give results for F^{SR} which are far from the ones produced by the other methods, such as dimensional continuation. In this paper, we will take the approach that the free energy is continuous at the long-range/short-range crossover.

where ψ is the digamma function. The sphere free energy in the quartic perturbed theory involves the same diagrams as in Figure 1 of [16]. Define

$$H_n = \int \prod_{i=1}^n d^d x_i \sqrt{g_{x_i}} \langle \phi_0^4(x_1) \cdots \phi_0^4(x_n) \rangle_0^{\text{conn}}. \quad (4.10)$$

Then we compute the free energy via

$$\delta F^{\text{LR}} = -\frac{\lambda_0^2}{2! 4^2} H_2 + \frac{\lambda_0^2}{3! 4^3} H_3 - \frac{\lambda_0^4}{4! 4^4} H_4, \quad (4.11)$$

where the H_n have the same combinatorial prefactors as in [16], but the diagrams have different singularities in ε . Details about the calculation of the free energy are provided in Appendix E.1.⁵

In three dimensions, we find at the fixed point

$$\tilde{F}^{\text{LR}} = N \tilde{F}_{\text{free}}^{\text{LR}} - \frac{N(N+2)}{(N+8)^2} \frac{\pi^2}{576} \left(\varepsilon^3 + \frac{3(5N+22)}{(N+8)^2} (2 - \pi + 4 \log 2) \varepsilon^4 \right) + \mathcal{O}(\varepsilon^5). \quad (4.12)$$

In two dimensions, the central charge is generally related to a -anomaly by $c = -3a$, and at the fixed point we find

$$c^{\text{LR}} = \frac{6}{\pi} N \tilde{F}_{\text{free}}^{\text{LR}} - \frac{N(N+2)}{8(N+8)^2} \left(\varepsilon^3 + \frac{12(5N+22) \log 2}{(8+N)^2} \varepsilon^4 \right) + \mathcal{O}(\varepsilon^5). \quad (4.13)$$

4.3 Cubic $O(N)$ model

We consider the cubic theory with a long-range kinetic term

$$S = \frac{2^{s-1} \Gamma(\frac{d+s}{2})}{\pi^{\frac{d}{2}} \Gamma(-\frac{s}{2})} \int d^d x d^d y \sqrt{g_x} \sqrt{g_y} \frac{\phi_0^i(x) \phi_0^i(y) + \sigma_0(x) \sigma_0(y)}{D(x, y)^{d+s}} + \int d^d x \sqrt{g_x} \left(\frac{g_{1,0}}{2} \sigma_0 \phi_0^i \phi_0^i + \frac{g_{2,0}}{6} \sigma_0^3 \right), \quad (4.14)$$

where $i = 1, \dots, N$ and we take $s = \frac{d+2\varepsilon}{3}$ so that ϕ_0^i and σ_0 have dimension $\frac{d-\varepsilon}{3}$ and the cubic perturbations are nearly marginal operators of dimension $d-\varepsilon$. Renormalized couplings are defined by

$$g_{i,0} = \mu^\varepsilon Z_{g_i} g_i, \quad Z_{g_i} = 1 + \frac{\delta_{g_i}}{g_i}, \quad i = 1, 2. \quad (4.15)$$

Note again that the scalar fields themselves are not renormalized in the long-range model. This fact makes the calculation of δ_{g_i} from corrections to the three-point vertex straightforward, and we

⁵Note that in the quartic long-range model in two and three dimensions, the only possible curvature counterterm that can appear is \mathcal{R} in two dimensions. We find a ε^{-1} divergence of F^{LR} beginning at order λ^3 in two dimensions, which could be renormalized by the \mathcal{R} counterterm. However, because we work strictly in two dimensions and the divergences do not enter the coefficient of $\log R$, this renormalization does not affect c .

include the details in Appendix E.2. The resulting beta functions are

$$\beta_1 = -\varepsilon g_1 - \frac{2g_1^2(g_1 + g_2)}{(4\pi)^{\frac{d}{2}}\Gamma(\frac{d}{2})}, \quad \beta_2 = -\varepsilon g_2 - \frac{2(Ng_1^3 + g_2^3)}{(4\pi)^{\frac{d}{2}}\Gamma(\frac{d}{2})}. \quad (4.16)$$

To compute the free energy to order ε^2 , we consider the same diagrams up to four points as in (3.3):

$$\delta F^{\text{LR}} = -\frac{G_2}{2!(3!)^2} - \frac{G_4}{4!(3!)^4}, \quad (4.17)$$

where the combinatorial factors of each term are the same as in dimensional regularization, but the integrals have different singularities in the long-range model. They are evaluated for various dimensions d in Appendix E.2. In the long-range cubic model, there are possible curvature counterterms in even dimensions, as well as a possible $\sigma\mathcal{R}$ vertex in three dimensions. As discussed in the previous subsection, the curvature counterterms in even dimensions do not affect the log R terms in the free energy, and we do not need to consider them to discuss a and c . In three dimensions, we check that the σ one-point function does not have any divergences to order $\mathcal{O}(g_i^3)$ (the diagram \mathcal{A}_3 in Figure 2.3 is finite) and therefore does not contribute to the free energy at order ε^2 . For $N = 0$ at the fixed point, we have

$$\begin{aligned} \tilde{F}^{\text{LR}} &= \tilde{F}_{\text{free}}^{\text{LR}} + \frac{\varepsilon^2}{288}, & d = 3, \\ a^{\text{LR}} &= \frac{2}{\pi} \tilde{F}_{\text{free}}^{\text{LR}} + \frac{\Gamma(\frac{7}{6})^3}{144\pi^{3/2}} \varepsilon^2, & d = 4, \\ \tilde{F}^{\text{LR}} &= \tilde{F}_{\text{free}}^{\text{LR}} + \frac{\Gamma(\frac{4}{3})^3}{960} \varepsilon^2, & d = 5. \end{aligned} \quad (4.18)$$

The case of $N = -2$ is also presented at the fixed point in (E.14) of Appendix E.2.

5 Numerical results for the sphere free energy

In this section, we compare numerical results for the free energy using dimensional continuation and the long-range approach. We consider quartic theories for small N in the first subsection, and various choices of N in cubic theories in the following subsections.

5.1 Quartic models

We compute \tilde{F}^{LRA} , the free energy at the fixed point in the long-range model corresponding to the $d = 3$ short-range result by taking $s_* = 3 - 2\Delta_\phi^{\text{SR}}$ and $\varepsilon_* = 2s_* - 3$ using bootstrap results [84] for Δ_ϕ^{SR} . For $N = 1$, $\Delta_\phi^{\text{SR}} = 0.5181$, for $N = 2$, $\Delta_\phi^{\text{SR}} = 0.5191$, and for $N = 3$, $\Delta_\phi^{\text{SR}} = 0.5189$. The corresponding value \tilde{F}^{LRA} is presented in the third line of Table 5.1. Here and in subsequent subsections, we find that using the exact value $\tilde{F}_{\text{free}}^{\text{LRA}}$ for the free field contribution gives the most

sensible results.⁶ We then add to that the contribution of the interactions $\delta\tilde{F}^{\text{LR}}$, evaluated at $\varepsilon = \varepsilon_*$ (we do not use Padé approximants in this case as they appear to have poles). We also compare the result of the long-range approach to the fuzzy sphere [22] and the ε -expansion [16] in Table 5.1. Note that in the fourth line, we use the result of the two-sided Padé approximants in Table 1 of [16] for $\tilde{F}_{\text{Ising}}^{\text{Padé}}$.

Quantity	$N = 1$	$N = 2$	$N = 3$
$N\tilde{F}_{\text{free}}$	0.06381	0.1276	0.1914
$N\tilde{F}_{\text{free}}^{\text{LRA}}$	0.06361	0.1272	0.1908
\tilde{F}^{LRA}	0.06234	0.1245	0.1868
$\tilde{F}_{\text{Ising}}^{\text{Padé}}$ [16]	0.06223	0.1243	0.1866
\tilde{F} fuzzy sphere [22]	0.0612	–	–

Table 5.1: Comparison of \tilde{F} in the $d = 3$ quartic model in several methods. In three dimensions $\tilde{F} = F$. The exact value of $\tilde{F}_{\text{free}} = \frac{\log 2}{8} - \frac{3\zeta(3)}{16\pi^2}$ in the first line is from (3.1), the second line is the exact value $\tilde{F}_{\text{free}}^{\text{LRA}}$ from (4.6) at $s = s_*$, the third line is the result of the long-range approach (4.12), and the fourth and fifth lines are ε -expansion results from [16] and fuzzy sphere results from [22].

Quantity	$N = 1$	$N = 2$
Nc_{free}	1	2
$Nc_{\text{free}}^{\text{LRA}}$	0.66992	1.3398
c^{LRA}	0.58931	1.1714
c (exact)	$\frac{1}{2}$	1

Table 5.2: Comparison of c in the quartic model from various results. In two dimensions we use $c = -3a$. The first line is the exact free value using (3.1), the second line uses the exact free value $\tilde{F}_{\text{free}}^{\text{LRA}}$ from (4.6) at $s = s_*$, the third line is the result of the long-range approach (4.13), and the fourth line is the exact value.

In two dimensions, we can evaluate (4.13) at ε_* corresponding to the exact value of $\Delta_\phi^{\text{SR}} = \frac{1}{8}$ for $N = 1, 2$ [85] in $d = 2$, $s_* = 2 - 2\Delta_\phi^{\text{SR}}$ and $\varepsilon_* = 2s_* - 2$ and compare this to the exact result in Table 5.2. Figures 5.1 and 5.2 show results for \tilde{F} in the $N = 1$ and $N = 2$ quartic theories, respectively, between two and four dimensions. In Figure 5.1, we present the [3, 3] Padé approximant from [16] as $\tilde{F}_{\text{Ising}}^{\text{Padé}}$. In Figure 5.2, following [16], we present the [4, 2] Padé approximant of the expanded $f(\varepsilon) = \tilde{F}_{\text{free}}(4 - \varepsilon) + \delta\tilde{F}$, then add one copy of the exact value \tilde{F}_{free} to obtain $\tilde{F}_{O(2)}^{\text{Padé}}$.

⁶By exact value, we mean substituting s_* into (4.6) and numerically evaluating the integral. In contrast, we can obtain an ε -expansion of $\tilde{F}_{\text{free}}^{\text{LR}}$ using $\varepsilon = 2s - 3$. For example, keeping terms up to ε^3 , we have in $3d$

$$\tilde{F}_{\text{free}}^{\text{LR}} = 0.04234 + 0.03068\varepsilon - 0.0005747\varepsilon^2 - 0.005878\varepsilon^3 + \mathcal{O}(\varepsilon^4) .$$

Combining this with the leading order correction $\delta\tilde{F}^{\text{LR}} = -0.00063462\varepsilon^3 + \mathcal{O}(\varepsilon^4)$ yields $\tilde{F}^{\text{LRA}} \approx 0.0651$ for $N = 1$, which is bigger than \tilde{F}_{free} . This \tilde{F}^{LRA} is not a good approximation for Ising model since it violates the F -theorem. On the other hand, the F -theorem is automatically satisfied if we use the exact value of $\tilde{F}_{\text{free}}^{\text{LRA}}$.

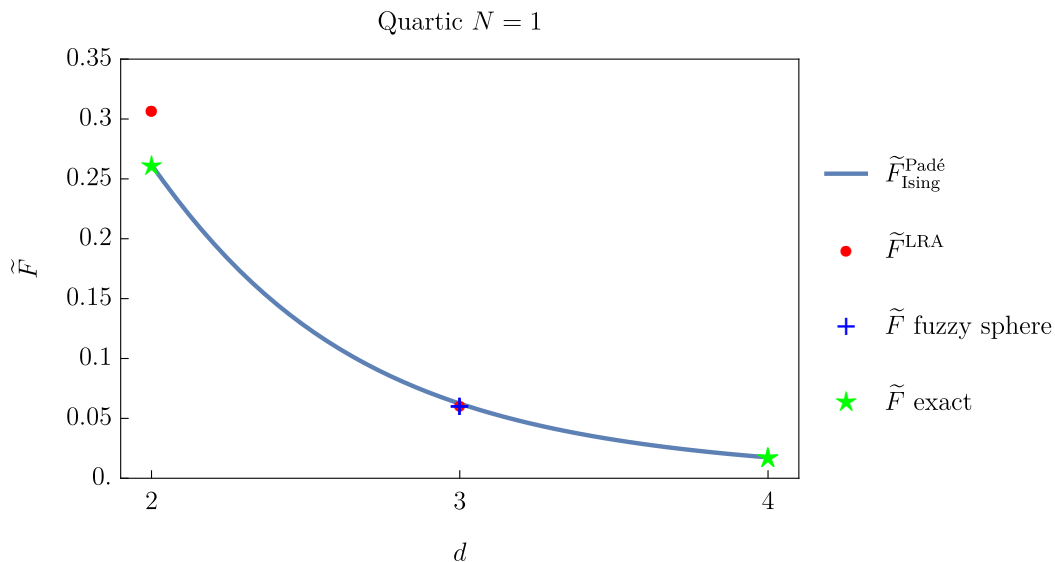


Figure 5.1: Free energy in $N = 1$ quartic theory between two and four dimensions. The blue line is the ϵ -expansion result $\tilde{F}_{\text{Ising}}^{\text{Padé}}$ [16] based on a two-sided Padé approximation, the red dots are the results of the long-range approach \tilde{F}^{LRA} , the blue cross is the fuzzy sphere result, and the green stars are the exact results in two ($\frac{\pi}{12}$) and four ($\frac{\pi}{180}$) dimensions.

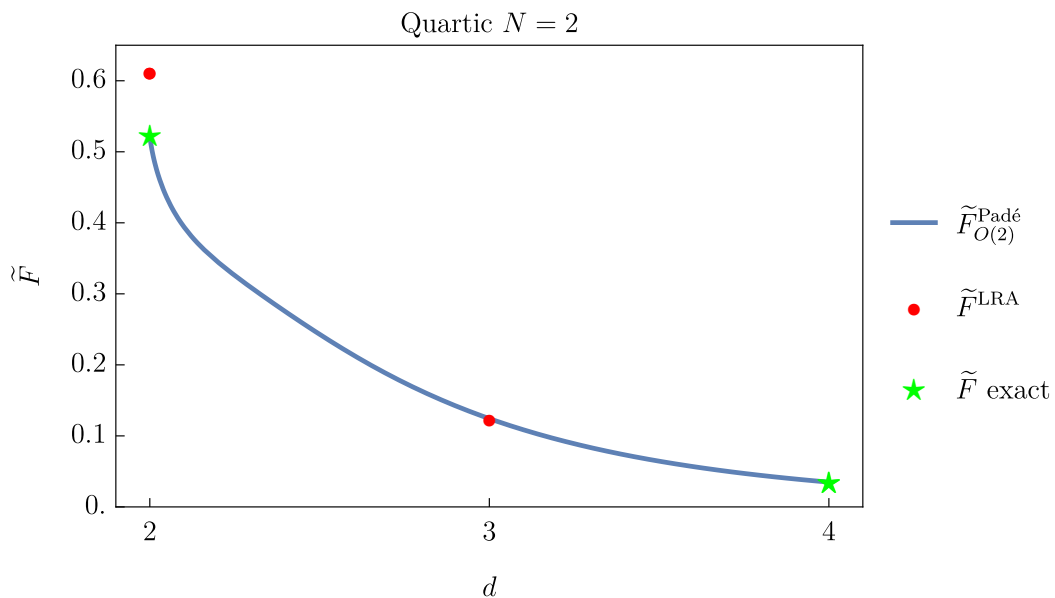


Figure 5.2: Free energy numerics in $N = 2$ quartic theory between two and four dimensions. The solid blue line is the ϵ -expansion result $\tilde{F}_{O(2)}^{\text{Padé}}$ [16] based on a two-sided Padé approximation, the red dots are the results of the long-range approach \tilde{F}^{LRA} , and the green stars are the exact results in two ($\frac{\pi}{6}$) and four ($\frac{\pi}{90}$) dimensions.

5.2 Cubic Lee-Yang model ($N = 0$)

The $N = 0$ case of the cubic $O(N)$ model, which has applications to the Lee-Yang edge singularity and percolation theory, was considered (aside from studies of general N) in flat space by [25, 26, 31, 51–54] and on the sphere by [66, 67, 86–90]. See also [91] for a recent review. In $d = 2$ the Lee-Yang model corresponds to the $M(2, 5)$ minimal model with central charge $c(2, 5) = -\frac{22}{5}$ [32] and corresponding free energy $\tilde{F}_{\text{YL}} = \frac{\pi}{6}c(2, 5)$. Using the expansion (3.5) with $N = 0$ near $d = 6$, and the exact value at $d = 2$, we have:

$$\tilde{F}_{\text{YL}}(d) = \begin{cases} -\frac{11\pi}{15}, & d = 2, \\ \tilde{F}_{\text{free}}(6 - \epsilon) + \frac{\pi\epsilon^2}{25920} + \frac{397\pi\epsilon^3}{7873200} + \mathcal{O}(\epsilon^4), & d = 6 - \epsilon, \end{cases} \quad (5.1)$$

where $\tilde{F}_{\text{free}}(6 - \epsilon)$ denotes the expansion of \tilde{F}_{free} to order ϵ^3 (C.3). We can construct a Padé approximant to the generalized free energy near $d = 6$:

$$\tilde{F}^{[m,n]}(\epsilon) = \frac{A_0 + A_1\epsilon + \dots + A_m\epsilon^m}{1 + B_1\epsilon + \dots + B_n\epsilon^n}, \quad (5.2)$$

where $m + n \leq 3$, which agrees with the known terms to order ϵ^3 but is expected to provide a better approximation of \tilde{F} . In principle, the approximation can be improved by imposing the known boundary condition at $d = 2$. However, we find that doing so leads to approximants with poles in the denominator. Still, applying the one-point Padé approximant to \tilde{F}_{YL} at $d = 6$, we find that the [1,2] Padé has no poles:

$$\tilde{F}_{\text{YL}}^{[1,2]} = \frac{0.00207777 + 0.000500993\epsilon}{1 - 0.742084\epsilon + 0.159126\epsilon^2}. \quad (5.3)$$

Values for various choices of ϵ (choices of d) are presented in the last line of Table 5.3. It is difficult to extrapolate to $d = 2$ with the ϵ expansion, and we do not include it in the numerics.

In the long-range cubic model with $N = 0$, we can evaluate the long-range free energy at the value $\varepsilon_* = \frac{3s_* - d}{2}$ with $s_* = d - 2\Delta_\sigma^{\text{SR}}$ with $\Delta_\sigma^{\text{SR}}$ at the short-range crossover derived from bootstrap results [92].⁷ We compare the result of the long-range approach to the ϵ expansion in Table 5.3 and Figure 5.3.

In Table 5.3, \tilde{F} denotes $-F$ in five dimensions, $\frac{\pi}{2}a$ in four dimensions, and F in three dimensions. The first line is the exact value of \tilde{F}_{free} in each dimension from (3.1), the second line is the exact value $\tilde{F}_{\text{free}}^{\text{LRA}}$ in each dimension from (4.6) at $s = s_*$, the third line is the result of the long-range approach (4.18) and the last line is the Padé approximant in the ϵ -expansion (5.3).

Note that the exact value of the central charge is $c = -\frac{22}{5}$ in $d = 2$. In the long-range approach

⁷Table 2 of [92] gives the edge exponent $\sigma(d)$, which is related to $\Delta_\sigma^{\text{SR}}$ by $\Delta_\sigma^{\text{SR}} = d \frac{\sigma(d)}{1 + \sigma(d)}$. In five dimensions $\Delta_\sigma^{\text{SR}} = 1.46$, in four dimensions $\Delta_\sigma^{\text{SR}} = 0.847$, and in three dimensions $\Delta_\sigma^{\text{SR}} = 0.235$. These are close to the results of the five-loop calculation presented in [26].

in three dimensions, \tilde{F}^{LR} is slightly negative, lower than the corresponding $6 - \epsilon$ expansion result.

Dimension	$d = 5$	$d = 4$	$d = 3$
\tilde{F}_{free}	0.0057430	0.017453	0.063807
$\tilde{F}_{\text{free}}^{\text{LRA}}$	0.0056606	0.013515	-0.026403
\tilde{F}^{LRA}	0.0059593	0.016848	-0.0081155
$\tilde{F}_{\text{YL}}^{[1,2]}$	0.020218	0.012871	0.017393

Table 5.3: Free energy in $N = 0$ cubic Lee-Yang theory. \tilde{F} denotes $-F$ in five dimensions, $\frac{\pi}{2}a$ in four dimensions, and F in three dimensions. The first line is the exact value of \tilde{F}_{free} in each dimension from (3.1), the second line is the exact value $\tilde{F}_{\text{free}}^{\text{LRA}}$ in each dimension from (4.6) at $s = s_*$, the third line is the result of the long-range approach (4.18), and the last line is the Padé approximant in the ϵ -expansion (5.3).

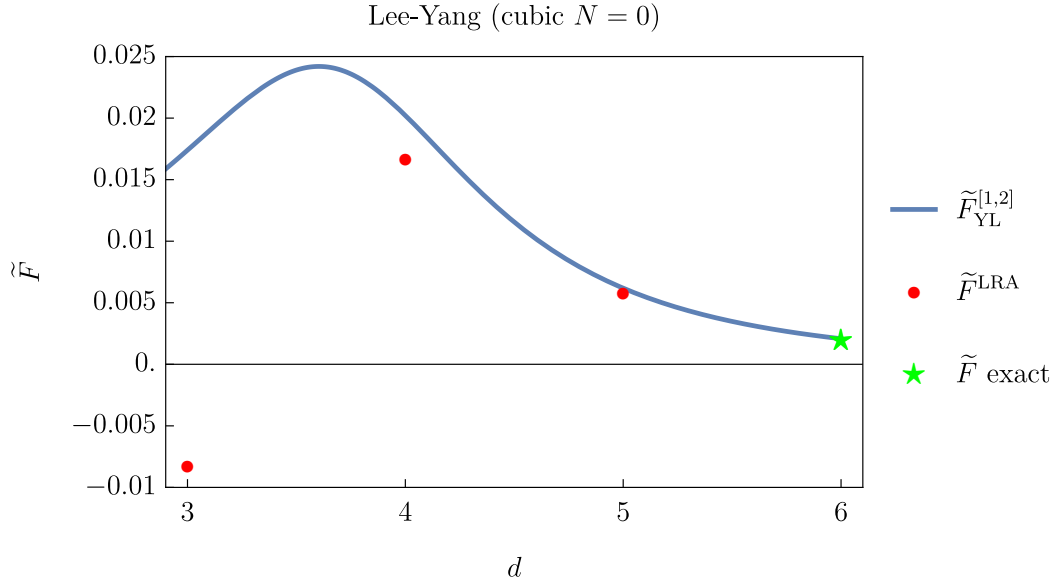


Figure 5.3: Free energy numerics in $N = 0$ cubic Lee-Yang theory in various dimensions. The solid blue line is the ϵ -expansion result $\tilde{F}_{\text{YL}}^{[1,2]}$ and the red dots are the results of the long-range approach \tilde{F}^{LRA} . The green star is the exact value ($\frac{\pi}{1512}$) in six dimensions (C.3).

5.3 $OSp(1|2)$ model (cubic $N = -2$)

In this subsection we consider the cubic $OSp(1|2)$ model on a sphere in $d = 6 - \epsilon$ dimensions. The $Sp(N)$ model in flat space was proposed in [37], where the leading term in the ϵ -expansion of the free energy was computed and for $N = 2$ it was shown that the IR fixed point possesses an enhanced global symmetry given by the supergroup $OSp(1|2)$. A more general class of critical field theories with $OSp(1|2M)$ symmetry was studied in [38]. The bare action of the $Sp(2)$ model,

including curvature couplings on the sphere, is

$$S = \int d^d x \sqrt{g} \left(\partial_\mu \theta_0 \partial^\mu \bar{\theta}_0 + \frac{1}{2} (\partial_\mu \sigma_0)^2 + \frac{\xi}{2} \mathcal{R} (\sigma_0^2 + 2\theta_0 \bar{\theta}_0) + g_{1,0} \sigma_0 \theta_0 \bar{\theta}_0 + \frac{1}{6} g_{2,0} \sigma_0^3 + \right. \\ \left. + \eta_{1,0} \mathcal{R} \theta_0 \bar{\theta}_0 + \frac{\eta_{2,0}}{2} \mathcal{R} \sigma_0^2 + \kappa_0 \mathcal{R}^2 \sigma_0 + b_0 \mathcal{R}^3 \right), \quad (5.4)$$

where θ is a complex anticommuting scalar. For $g_{2,0} = 2g_{1,0}$, $\eta_{1,0} = \eta_{2,0}$, $\kappa_0 = 0$ this action possesses a fermionic symmetry with a complex anti-commuting scalar parameter α [37]

$$\delta \theta = \sigma \alpha, \quad \delta \bar{\theta} = \sigma \bar{\alpha}, \quad \delta \sigma = -\alpha \bar{\theta} + \bar{\alpha} \theta \quad (5.5)$$

that enhances $Sp(2)$ to $OSp(1|2)$, which is the smallest supergroup. As a consequence of this symmetry, the scaling dimensions of σ and θ are equal, there is a single cubic coupling g_0 and quadratic curvature coupling η_0 , and a linear κ_0 curvature coupling is forbidden. The beta functions for this theory in $d = 6 - \epsilon$ are related to the beta functions of the cubic $O(N)$ theory (2.13) via the replacement $N = 2 \rightarrow -N = -2$, and specializing to $g \equiv g_2 = 2g_1$, $\eta = \eta_1 = \eta_2$, and $\kappa = 0$. Note that β_κ vanishes exactly in this model, which we check holds to the order we compute in (2.29).

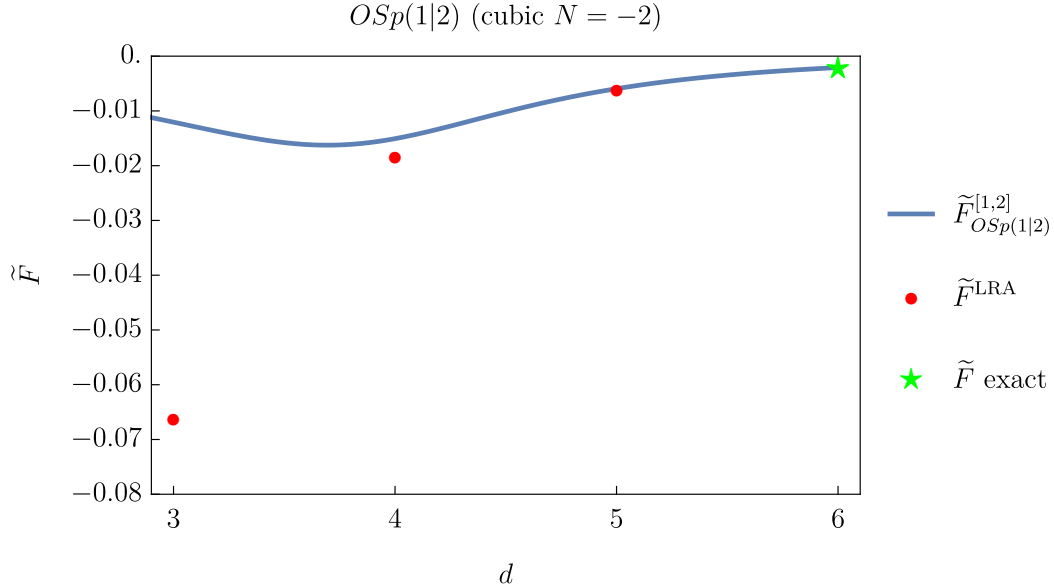


Figure 5.4: Free energy numerics in $N = -2$ theory $OSp(1|2)$ theory in various dimensions. The solid blue line is the ϵ -expansion result $\tilde{F}_{OSp(1|2)}^{[1,2]}$ and the red dots are results of the long-range approach \tilde{F}^{LRA} . The green star is the exact value ($-\frac{\pi}{1512}$) in six dimensions.

From the result for general N , we find the the generalized free energy at $d = 6 - \epsilon$:

$$\tilde{F}_{OSp(1|2)} = -\tilde{F}_{\text{free}} - \frac{\pi \epsilon^2}{43200} - \frac{169 \pi \epsilon^3}{5832000} + \mathcal{O}(\epsilon^4). \quad (5.6)$$

Applying the one-sided Padé approximant at $d = 6$ to $\tilde{F}_{OSp(1|2)}$, we find that the [1,2] Padé has no poles:

$$\tilde{F}_{OSp(1|2)}^{[1,2]} = -\frac{0.00207777 + 0.000539773\epsilon}{1 - 0.723420\epsilon + 0.164109\epsilon^2}. \quad (5.7)$$

In the long-range cubic model with $N = -2$, we can compute the free energy at the values ϵ_*, s_* derived from Monte Carlo results in [40] for $\Delta_\sigma^{\text{SR}} = \Delta_\theta^{\text{SR}}$.⁸ We compare these results to the $6 - \epsilon$ expansion in Table 5.4 and Figure 5.4. The table is set up in parallel with Table 5.3.

Dimension	$d = 5$	$d = 4$	$d = 3$
$-\tilde{F}_{\text{free}}$	-0.0057430	-0.0174531	-0.06381
$-\tilde{F}_{\text{free}}^{\text{LRA}}$	-0.005678	-0.01650	-0.05849
\tilde{F}^{LRA}	-0.005868	-0.01810	-0.06599
$\tilde{F}_{OSp(1 2)}^{[1,2]}$	-0.0059400	-0.00150639	-0.012054

Table 5.4: Free energy in $OSp(1|2)$ model. Here, \tilde{F} denotes $-F$ in five dimensions, $\frac{\pi}{2}a$ in four dimensions, and F in three dimensions. The first line is the exact value of \tilde{F}_{free} in each dimension from (3.1), the second line is the exact value $\tilde{F}_{\text{free}}^{\text{LRA}}$ in each dimension from (4.6) at $s = s_*$, the third line is the result of long-range approach (E.14), and the last line is the Padé approximant in the ϵ -expansion (5.7).

Note that the exact value in two dimensions is $c = -2$, which corresponds to $\tilde{F} = -1.0472$. The long-range calculation is closer to this value in 3d than the ϵ -expansion, and gives points monotonically varying with dimension.

5.4 Cubic $N = 1$ model

The $N = 1$ cubic model corresponds in $d = 2$ to the D_5 modular invariant of $M(3, 8)$ minimal model with central charge $c(3, 8) = -\frac{21}{4}$, and the corresponding free energy $\tilde{F}_{\text{cubic } N=1} = \frac{\pi}{6}c(3, 8)$ [24, 33, 35]. Using the expansion (3.5) near $d = 6$ with $N = 1$ and the exact value at $d = 2$, we have:⁹

$$\tilde{F}_{\text{cubic } N=1}(d) = \begin{cases} -\frac{7\pi}{8}, & d = 2, \\ 2\tilde{F}_{\text{free}}(6 - \epsilon) + \frac{37\pi\epsilon^2}{479040} + \frac{180905801\pi\epsilon^3}{1789221585600} + \mathcal{O}(\epsilon^4), & d = 6 - \epsilon. \end{cases} \quad (5.8)$$

Again, the two-sided Padé imposed with the boundary condition at $d = 2$ leads to poles in the denominator. Applying the one-sided Padé approximant to $\tilde{F}_{\text{cubic } N=1}$, we find that the [1,2] Padé has no poles:

$$\tilde{F}_{\text{cubic } N=1}^{[1,2]} = \frac{0.00415555 + 0.00100299\epsilon}{1 - 0.741842\epsilon + 0.158829\epsilon^2}, \quad (5.9)$$

⁸Table I of [40] gives γ/ν for $q = 0$, from which we compute $\Delta_\sigma^{\text{SR}} = \Delta_\theta^{\text{SR}} = \frac{d}{2} - \frac{\gamma}{2\nu}$ [38]. In five dimensions $\Delta_\sigma^{\text{SR}} = 1.46$, in four dimensions $\Delta_\sigma^{\text{SR}} = 0.920$, and in three dimensions $\Delta_\sigma^{\text{SR}} = -0.0838$.

⁹In the long-range approach, there appears to be no fixed point corresponding to the $M(3, 8)$ universality class. Therefore, this method cannot be used to estimate the sphere free energy.

where we present the result at various d in Table 5.5 and Figure 5.5.

Dimension	$d = 5$	$d = 4$	$d = 3$
$2\tilde{F}_{\text{free}}$	0.011486	0.034907	0.127614
$\tilde{F}_{\text{cubic } N=1}^{[1,2]}$	0.012371	0.040635	0.035131

Table 5.5: $6 - \epsilon$ expansion for $N = 1$ cubic theory. Here, \tilde{F} denotes $-F$ in five dimensions, $\frac{\pi}{2}a$ in four dimensions, and F in three dimensions. The first line uses the exact value of \tilde{F}_{free} in each dimension from (3.1), and the second line uses the Padé approximant (5.9).

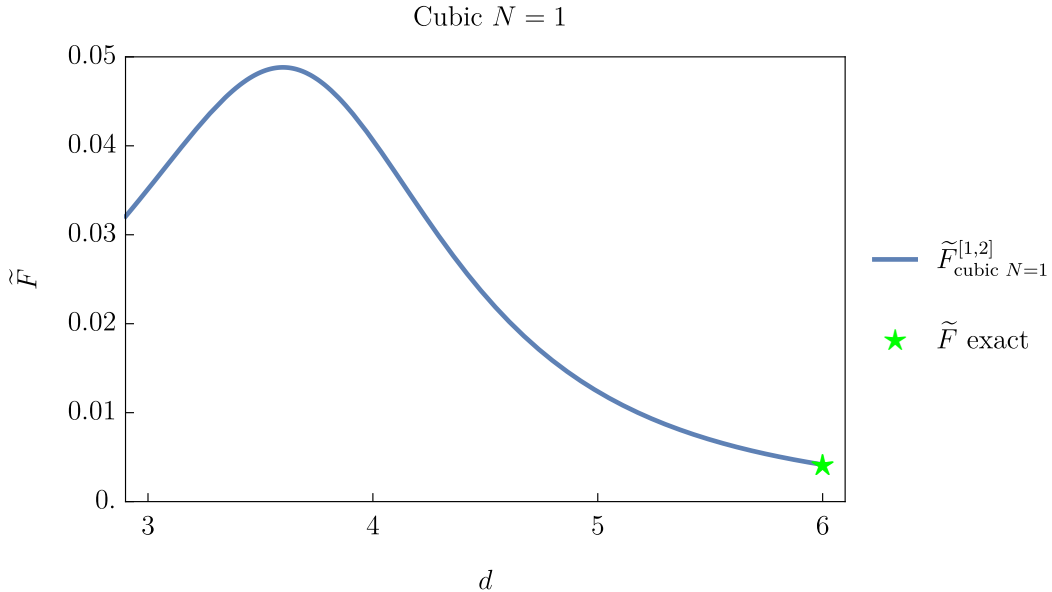


Figure 5.5: Free energy numerics in $N = 1$ cubic theory in various dimensions. The solid blue line is the ϵ -expansion result $\tilde{F}_{\text{cubic } N=1}^{[1,2]}$ and the green star is the exact value ($\frac{\pi}{756}$) in six dimensions.

In [24, 33, 35] the RG flow $M(3, 10) + \phi_{1,7} \rightarrow M(3, 8)$ between the D -series modular invariants of two non-unitary minimal models was studied. The D_6 modular invariant of $M(3, 10)$ describes a pair of the Yang-Lee models $M(2, 5)$ [93–95]. Let us find the change in \tilde{F} along the RG flow from $2\tilde{F}_{\text{YL}}$ to $\tilde{F}_{\text{cubic } N=1}$:

$$\begin{aligned}
 2\tilde{F}_{\text{YL}} - \tilde{F}_{\text{cubic } N=1} &= \frac{\pi\epsilon^2}{12934080} + \frac{1018225963\pi\epsilon^3}{3913027607707200} + \mathcal{O}(\epsilon^4) \\
 &= 2.42893 \cdot 10^{-7}\epsilon^2 + 8.17488 \cdot 10^{-7}\epsilon^3 + \mathcal{O}(\epsilon^4) > 0.
 \end{aligned}
 \tag{5.10}$$

Since this change is positive, the generalized F -theorem [16], which conjectures that the generalized free energy \tilde{F} decreases along RG flows between unitary theories, is violated for these non-unitary theories.

Acknowledgements

We are grateful to L. Fei and G. Tarnopolsky for collaboration at very early stages of this project. We also thank G. Tarnopolsky for very useful discussions. This work was supported in part by the US National Science Foundation Grant No. PHY-2209997 and by the Simons Foundation Grant No. 917464.

A Flat space renormalization

In this appendix, we summarize previous results for the flat-space renormalization of the cubic $O(N)$ model. In minimal subtraction, the counterterms (2.3) have the structure

$$\delta_{\phi,\sigma} = \sum_{n=1}^{\infty} \frac{\delta_{\phi,\sigma}^{(n)}(g_1, g_2)}{\epsilon^n}, \quad \delta_{g_1, g_2} = \sum_{n=1}^{\infty} \frac{\delta_{g_1, g_2}^{(n)}(g_1, g_2)}{\epsilon^n}. \quad (\text{A.1})$$

In perturbation theory, powers of g_1 and g_2 appear as follows:

$$\delta_{\phi,\sigma}^{(n)} = \sum_k \delta_{\phi,\sigma}^{(n,2k)}, \quad \delta_{g_1, g_2}^{(n)} = \sum_k \delta_{g_1, g_2}^{(n,2k+1)}, \quad \{\delta_{\phi,\sigma}^{(n,k)}, \delta_{g_1, g_2}^{(n,k)}\} \propto g_1^i g_2^j, \quad i + j = k. \quad (\text{A.2})$$

The one-loop result was first obtained in [23], then the three-loop result in [24] and four-loop result in [25]. The five-loop result for $N = 0$ was computed in [26]. We use the two-loop counterterms:

$$\delta_{\phi}^{(1,2)} = -\frac{g_1^2}{3(4\pi)^3}, \quad \delta_{\phi}^{(1,4)} = \frac{g_1^2(g_1^2(11N - 26) - 48g_1g_2 + 11g_2^2)}{432(4\pi)^6}, \quad (\text{A.3})$$

$$\delta_{\sigma}^{(1,2)} = -\frac{Ng_1^2 + g_2^2}{6(4\pi)^3}, \quad \delta_{\sigma}^{(1,4)} = -\frac{2Ng_1^4 + 48Ng_1^3g_2 - 11Ng_1^2g_2^2 + 13g_2^4}{432(4\pi)^6}, \quad (\text{A.4})$$

and two-loop wavefunction renormalization

$$Z_{\phi} = 1 - \frac{g_1^2}{3(4\pi)^3\epsilon} - \frac{g_1^2(g_1^2(N - 10) - 12g_1g_2 + g_2^2)}{36(4\pi)^6\epsilon^2} + \frac{g_1^2(g_1^2(11N - 26) - 48g_1g_2 + 11g_2^2)}{432(4\pi)^6\epsilon}, \quad (\text{A.5})$$

$$Z_{\sigma} = 1 - \frac{Ng_1^2 + g_2^2}{6(4\pi)^3\epsilon} + \frac{4Ng_1^4 + 12Ng_1^3g_2 - Ng_1^2g_2^2 + 5g_2^4}{36(4\pi)^6\epsilon^2} - \frac{2Ng_1^4 + 48Ng_1^3g_2 - 11Ng_1^2g_2^2 + 13g_2^4}{432(4\pi)^6\epsilon}. \quad (\text{A.6})$$

The beta-functions for the cubic $O(N)$ model were computed in [23–25]. At two loops,

$$\beta_{g_1} = -\frac{\epsilon}{2}g_1 + \frac{g_1((N-8)g_1^2 - 12g_1g_2 + g_2^2)}{12(4\pi)^3} - \frac{g_1((86N+536)g_1^4 - 12(11N-30)g_1^3g_2 + (11N+628)g_1^2g_2^2 + 24g_1g_2^3 - 13g_2^4)}{432(4\pi)^6}, \quad (\text{A.7})$$

$$\beta_{g_2} = -\frac{\epsilon}{2}g_2 - \frac{4Ng_1^3 - Ng_1^2g_2 + 3g_2^3}{4(4\pi)^3} - \frac{24Ng_1^5 + 322Ng_1^4g_2 + 60Ng_1^3g_2^2 - 31Ng_1^2g_2^3 + 125g_2^5}{144(4\pi)^6}. \quad (\text{A.8})$$

We also have the two-loop relation between bare and renormalized couplings

$$g_{1,0} = \mu^{\epsilon/2} \left(g_1 + \frac{g_1((N-8)g_1^2 - 12g_1g_2 + g_2^2)}{12(4\pi)^3\epsilon} - \frac{g_1((86N+536)g_1^4 - 12(11N-30)g_1^3g_2 + (11N+628)g_1^2g_2^2 + 24g_1g_2^3 - 13g_2^4)}{864(4\pi)^6\epsilon} + \frac{g_1((N(80+3N) + 352)g_1^4 + 24(28-5N)g_1^3g_2 + 10(N+24)g_1^2g_2^2 + 72g_1g_2^3 - 17g_2^4)}{288(4\pi)^6\epsilon^2} \right), \quad (\text{A.9})$$

$$g_{2,0} = \mu^{\epsilon/2} \left(g_2 - \frac{4Ng_1^3 - Ng_1^2g_2 + 3g_2^3}{4(4\pi)^3\epsilon} - \frac{24Ng_1^5 + 322Ng_1^4g_2 + 60Ng_1^3g_2^2 - 31Ng_1^2g_2^3 + 125g_2^5}{288(4\pi)^6\epsilon} + \frac{24N(4-N)g_1^5 + N(5N+128)g_1^4g_2 + 72Ng_1^3g_2^2 - 34Ng_1^2g_2^3 + 81g_2^5}{96(4\pi)^6\epsilon^2} \right). \quad (\text{A.10})$$

For reference, we include the fixed points in $d = 6 - \epsilon$ for the specific N included in Section 3:

$$\begin{aligned} N = 0: \quad g_2^* &= i\sqrt{\frac{2(4\pi)^3\epsilon}{3}} \left(1 + \frac{125}{324}\epsilon + \mathcal{O}(\epsilon^2) \right), \quad g_1^* = 0, \\ N = -2: \quad g_2^* &= 2g_1^* = i\sqrt{\frac{4(4\pi)^3\epsilon}{5}} \left(1 + \frac{67}{180}\epsilon + \mathcal{O}(\epsilon^2) \right), \\ N = 1: \quad \begin{cases} g_1^* &= 40i\sqrt{\frac{6\pi^3\epsilon}{499}} \left(1 + \frac{2633149}{7470036}\epsilon + \mathcal{O}(\epsilon^2) \right), \\ g_2^* &= 48i\sqrt{\frac{6\pi^3\epsilon}{499}} \left(1 + \frac{227905}{498002}\epsilon + \mathcal{O}(\epsilon^2) \right). \end{cases} \end{aligned} \quad (\text{A.11})$$

Note that for $N = 1$ there is also an unstable fixed point when $g_1^* = g_2^*$, which is the sum of two $N = 0$ theories [24]. We discuss the flow between them in Section 5.4.

B Integral conventions on the sphere

In this appendix, we review our conventions for computing Feynman integrals on sphere, following [16]. We use the conformally flat metric on the d -dimensional sphere of radius R :

$$ds^2 = \Omega(x)^2 dx^2, \quad \Omega(x) \equiv \frac{2R}{1+x^2}, \quad (\text{B.1})$$

where $x \in \mathbb{R}^d$. Its volume is

$$\text{Vol}(S^d) = \int d^d x \sqrt{g} = \frac{2\pi^{\frac{d+1}{2}} R^d}{\Gamma\left(\frac{d+1}{2}\right)}, \quad (\text{B.2})$$

and its Ricci scalar curvature is

$$\mathcal{R} = \frac{d(d-1)}{R^2}. \quad (\text{B.3})$$

The propagator \mathbb{G}_d for a massless scalar on \mathbb{R}^d is

$$\mathbb{G}_d(x, y) = \frac{C_d}{|x-y|^{d-2}}, \quad C_d \equiv \frac{\Gamma\left(\frac{d}{2}-1\right)}{4\pi^{\frac{d}{2}}}. \quad (\text{B.4})$$

Because the sphere is conformally flat, the propagator G_d of a conformally coupled scalar on S^d is related to the propagator of a massless scalar on \mathbb{R}^d by the Weyl factor Ω :

$$G_d(x, y) = \frac{C_d}{D(x, y)^{d-2}}, \quad D(x, y) \equiv \sqrt{\Omega(x)\Omega(y)}|x-y|. \quad (\text{B.5})$$

Note that the function $D(x, y)$ is $SO(d+1)$ invariant. Two well-known exactly solvable integrals on sphere are [3, 5, 96]

$$I_2(\Delta) = \int \frac{d^d x d^d y \Omega^d(x) \Omega^d(y)}{D(x, y)^{2\Delta}} = 2^{1+d-2\Delta} \pi^{d+\frac{1}{2}} R^{2(d-\Delta)} \frac{\Gamma\left(\frac{d}{2}-\Delta\right)}{\Gamma\left(\frac{d+1}{2}\right)\Gamma(d-\Delta)}, \quad (\text{B.6})$$

$$I_3(\Delta) = \int \frac{d^d x d^d y d^d z \Omega^d(x) \Omega^d(y) \Omega^d(z)}{[D(x, y)D(y, z)D(z, x)]^\Delta} = 8\pi^{\frac{3(1+d)}{2}} R^{3(d-\Delta)} \frac{\Gamma\left(d-\frac{3\Delta}{2}\right)}{\Gamma\left(\frac{d+1-\Delta}{2}\right)^3 \Gamma(d)}. \quad (\text{B.7})$$

C Details of free energy calculations

In this appendix, we include a summary of the terms that contribute to the sphere free energy in the $O(N)$ cubic model at sixth order in $g_{1,0}$ and $g_{2,0}$, computed in [14].

The sphere free energy for a conformally coupled free scalar in dimensional regularization on S^d is [15, 80]:

$$F_{\text{free}} = -\frac{1}{\sin\left(\frac{\pi d}{2}\right)\Gamma(1+d)} \int_0^1 du u \sin(\pi u) \Gamma\left(\frac{d}{2}+u\right) \Gamma\left(\frac{d}{2}-u\right). \quad (\text{C.1})$$

Near every even d this expression has a simple pole, with coefficient that reproduces the known a -anomalies. In $d = 6 - \epsilon$,

$$F_{\text{free}} = -\frac{1}{756\epsilon} + \mathcal{O}(1). \quad (\text{C.2})$$

The expansion of $\tilde{F}_{\text{free}}(6 - \epsilon)$ is

$$\tilde{F}_{\text{free}}(6 - \epsilon) = \frac{\pi}{1512} + 0.002042876\epsilon + 0.001064155\epsilon^2 + 0.000396195\epsilon^3 + \dots \quad (\text{C.3})$$

The free energy (3.3) up to order ϵ^2 involves the diagrams

$$G_2 = 3!t_2C_d^3I_2 \left(\frac{3(d-2)}{2} \right), \quad (\text{C.4})$$

$$G_4 = 3(3!)^3(3t_{41}G_4^{(1)} + 2t_{42}G_4^{(2)}), \quad (\text{C.5})$$

$$G_6 = 15(3!)^5(18t_{61}G_6^{(1)} + 6t_{62}G_6^{(2)} + 9t_{63}G_6^{(3)} + 36t_{64}G_6^{(4)} + 24t_{65}G_6^{(5)} + 4t_{66}G_6^{(6)}), \quad (\text{C.6})$$

which are shown in Figure 4 of [14], where the t -coefficients are

$$t_2 = 3Ng_{1,0}^2 + g_{2,0}^2, \quad t_{41} = (N+4)Ng_{1,0}^4 + 2Ng_{1,0}^2g_{2,0}^2 + g_{2,0}^4, \quad (\text{C.7})$$

$$t_{42} = 3Ng_{1,0}^4 + 4Ng_{1,0}^3g_{2,0} + g_{2,0}^4, \quad (\text{C.8})$$

$$t_{61} = 4N(N+1)g_{1,0}^6 + N(N+4)g_{1,0}^4g_{2,0}^2 + 2Ng_{1,0}^2g_{2,0}^4 + g_{2,0}^6, \quad (\text{C.9})$$

$$t_{62} = 8Ng_{1,0}^6 + (Ng_{1,0}^2 + g_{2,0}^2)^3, \quad t_{63} = N^2g_{1,0}^4(2g_{1,0} + g_{2,0})^2 + 4Ng_{1,0}^3g_{2,0}^3 + g_{2,0}^6, \quad (\text{C.10})$$

$$t_{64} = N(N+4)g_{1,0}^6 + 2N(N+2)g_{1,0}^5g_{2,0} + Ng_{1,0}^4g_{2,0}^2 + 2Ng_{1,0}^3g_{2,0}^3 + Ng_{1,0}^2g_{2,0}^4 + g_{2,0}^6, \quad (\text{C.11})$$

$$t_{65} = N(N+3)g_{1,0}^6 + 6Ng_{1,0}^5g_{2,0} + 3Ng_{1,0}^4g_{2,0} + 2Ng_{1,0}^3g_{2,0}^3 + g_{2,0}^6, \quad (\text{C.12})$$

$$t_{66} = 6Ng_{1,0}^6 + 9Ng_{1,0}^4g_{2,0}^2 + g_{2,0}^6. \quad (\text{C.13})$$

Evaluating the diagrams in $d = 6 - \epsilon$ gives

$$G_4^{(k)} = C_d^6(2R)^{12-3d}\text{Vol}(S^d)e^{\frac{3\gamma_E}{2}(d-6)+\frac{\pi^2}{16}(d-6)^2}\pi^{\frac{3d}{2}} \begin{cases} \frac{1}{18\epsilon} + \frac{43}{162} + \frac{2857}{3888}\epsilon + \mathcal{O}(\epsilon^2), & k=1, \\ -\frac{1}{3\epsilon} - \frac{3}{2} - \frac{191}{48}\epsilon + \mathcal{O}(\epsilon^2), & k=2, \end{cases} \quad (\text{C.14})$$

$$G_6^{(k)} = C_d^9(2R)^{18-4d}\text{Vol}(S^d)e^{\frac{5\gamma_E}{2}(d-6)+\frac{\pi^2}{16}(d-6)^2}\pi^{\frac{5d}{2}} \begin{cases} -\frac{1}{54\epsilon^2} - \frac{389}{2592\epsilon} - \frac{87}{128} + \mathcal{O}(\epsilon), & k=1, \\ -\frac{1}{36\epsilon^2} - \frac{139}{648\epsilon} - \frac{3547}{3888} + \mathcal{O}(\epsilon), & k=2, \\ \frac{1}{384} + \mathcal{O}(\epsilon), & k=3, \\ \frac{1}{9\epsilon^2} + \frac{733}{864\epsilon} + \frac{4675}{1296} + \mathcal{O}(\epsilon), & k=4, \\ -\frac{1}{3\epsilon^2} - \frac{703}{288\epsilon} + \mathcal{O}(1), & k=5, \\ -\frac{5}{24\epsilon} + \frac{\zeta(3)}{8} - \frac{475}{288} + \mathcal{O}(\epsilon), & k=6. \end{cases} \quad (\text{C.15})$$

Note that these expressions include a small correction to [14], specifically the $\mathcal{O}(1)$ term in $G_6^{(3)}$ (which does not change the result for the free energy at the order considered in [14]). We present the calculation of $G_6^{(3)}$ as an example in the next subsection.

To renormalize the free energy to sixth order in g_1 and g_2 , we compute the contributions to F from G_2 , G_4 , and G_6 and use (A.9) and (A.10) to express these contributions in terms of renormalized couplings. Then, we fix the counterterms in b_0 to remove the divergences in the free energy of the conformally coupled scalar (C.1) as well as divergences in the terms in F of order $\mathcal{O}(g_1^{n_1} g_2^{n_2})$ with $n_1 + n_2 = 6$ [14]:

$$\delta_b^{(1)} = \frac{N+1}{756 \cdot 450(4\pi)^3} + b_{61}, \quad (\text{C.16})$$

where

$$b_{61} = \frac{N(2(43N+268)g_1^6 - 12(11N-32)g_1^5 g_2 + (11N+950)g_1^4 g_2^2 + 84g_1^3 g_2^3 - 44g_1^2 g_2^4) + 125g_2^6}{2^{12} 3^8 5^3 (4\pi)^{12}}. \quad (\text{C.17})$$

The beta function is then

$$\beta_b = \epsilon b + \frac{N+1}{756 \cdot 450(4\pi)^3} + 4b_{61} \quad (\text{C.18})$$

with fixed point

$$b^* = -\frac{N+1}{756 \cdot 450(4\pi)^3 \epsilon} - \frac{4b_{61}^*}{\epsilon}. \quad (\text{C.19})$$

After renormalization, we find the free energy up to fourth order in g_1 and g_2 , which is given at the fixed point by (3.5).

C.1 Analytic calculation of $G_6^{(3)}$

The (one-particle-reducible) diagram $G_6^{(3)} = \textcircled{\circ} \textcircled{\circ} \textcircled{\circ}$ admits a simple analytic evaluation. To show this, we focus on its irreducible component $\textcircled{\circ}$ which is denoted by \mathcal{A}_3 in Figure 2.3. It takes the following form:

$$\mathcal{A}_3 \equiv \int \prod_{i=1}^2 \left(d^d x_i \Omega^d(x_i) G_d(x_i, x_0) \right) G_d(x_1, x_2)^2. \quad (\text{C.20})$$

This integral is independent of x_0 due to the $SO(d+1)$ symmetry. Therefore we can set $x_0 = 0$ in the stereographic coordinates. After performing the inversion $x_i^\mu \rightarrow x_i^\mu/x_i^2$ for x_1 and x_2 , we find

$$\mathcal{A}_3 = (2R)^{8-2d} C_d^4 \int \prod_{i=1}^2 \frac{d^d x_i}{(1+x_i^2)^{3-\frac{d}{2}}} \frac{1}{x_{12}^{2(d-2)}}. \quad (\text{C.21})$$

The remaining integral has been studied in Appendix B of [14]. Following the notation of this paper, the result of \mathcal{A}_3 can be expressed as

$$\mathcal{A}_3 = (2R)^{8-2d} C_d^4 \Gamma_0 \left(3 - \frac{d}{2}, 3 - \frac{d}{2}, d - 2 \right) = -\frac{1}{8(4\pi)^6 R^4} + \mathcal{O}(\epsilon), \quad (\text{C.22})$$

where

$$\Gamma_0(a_1, a_2, b) = \frac{\pi^d \Gamma(\frac{d}{2} - b) \Gamma(a_1 + b - \frac{d}{2}) \Gamma(a_2 + b - \frac{d}{2}) \Gamma(a_1 + a_2 + b - d)}{\Gamma(\frac{d}{2}) \Gamma(a_1) \Gamma(a_2) \Gamma(a_1 + a_2 + 2b - d)}. \quad (\text{C.23})$$

The result for \mathcal{A}_3 first appeared in [96, 97]. Then, by gluing two copies of \mathcal{A}_3 , we get

$$\begin{aligned} G_6^{(3)} &= C_d \mathcal{A}_3^2 I_2 \left(\frac{d-2}{2} \right) = (2R)^{18-3d} C_d^9 \Gamma_0^2 \left(3 - \frac{d}{2}, 3 - \frac{d}{2}, d-2 \right) \Gamma_0 \left(1 + \frac{d}{2}, 1 + \frac{d}{2}, \frac{d-2}{2} \right) \\ &= (2R)^{18-4d} \text{Vol}(S^d) C_d^9 e^{\frac{5\gamma_E}{2}(d-6) + \frac{\pi^2}{16}(d-6)^2} \pi^{\frac{5d}{2}} \left(\frac{1}{384} + \frac{77\epsilon}{4608} + \mathcal{O}(\epsilon^2) \right), \end{aligned} \quad (\text{C.24})$$

which is finite in the $\epsilon \rightarrow 0$ limit.

D Comparison of cubic $N = 0$ curvature couplings to previous literature

In this appendix, we comment on differences between our results and those of previous calculations of cubic $N = 0$ curvature coupling renormalization. For clarity, we first restate our results for the curvature beta functions at $N = 0$ (with $g_1 \rightarrow 0, g_2 \rightarrow g, \eta_1 \rightarrow 0, \eta_2 \rightarrow \eta$):

$$\begin{aligned} \beta_\kappa &= \frac{\epsilon}{2} \kappa + \frac{\kappa g^2}{12(4\pi)^3} - \frac{\eta g}{30(4\pi)^3} + 0 \cdot g^3 + 0 \cdot g^5 + \dots, \\ \beta_\eta &= -\frac{5\eta g^2}{6(4\pi)^3} + 0 \cdot g^4 + \dots, \end{aligned} \quad (\text{D.1})$$

where the dots in β_κ denote terms at $\mathcal{O}(g^7)$ as well as curvature contributions beginning at $\mathcal{O}(\eta^2 g, \eta g^3, \kappa g^4)$ and the dots in β_η denote terms at $\mathcal{O}(g^6)$ as well as higher powers of curvature couplings beginning at $\mathcal{O}(\eta g^4)$. The renormalization of κ was calculated to one-loop order in [66] and two-loop order in [67] using the background field method, with the resulting beta function (in our conventions):¹⁰

$$\beta_\kappa = \frac{\epsilon}{2} \kappa + \frac{\kappa g^2}{12(4\pi)^3} - \frac{\eta g}{30(4\pi)^3} - \frac{161g^3}{2^5 3^4 5^3 (4\pi)^6} + \dots, \quad (\text{D.2})$$

where dots denote $\mathcal{O}(g^5)$ as well as terms of higher order in curvature couplings multiplied by powers of g . This differs from our result by the g^3 and g^5 terms, which we found to have vanished. The absence of a g^3 correction is because the diagram \mathcal{A}_3 is finite, as also first computed in [96, 97].

The renormalization of η_0 was considered to one-loop order in [66] and two-loop order in [67,

¹⁰The computation of β_κ involves the beta function of g . We believe that there is a typo in the two-loop counterterm of g in [67].

[86, 87] using the background field method.¹¹ In our conventions, the result of [86, 87] is:

$$\beta_\eta = -\frac{5\eta g^2}{6(4\pi)^3} - \frac{97}{108} \frac{\eta g^4}{(4\pi)^6} - \frac{1}{72} \frac{g^4}{(4\pi)^6} + \dots, \quad (\text{D.3})$$

where the dots denote terms of $\mathcal{O}(g^6)$ as well as higher powers of curvature couplings multiplied by powers of g . This agrees with [66] at one-loop, and with [67] at two-loops, except the latter has the opposite sign for the ηg^2 term. This differs from ours by the g^4 term, which we found to be zero.

Note that it is not the case that $\beta_\eta = \gamma_{\sigma^2} \eta$, where γ_{σ^2} is defined in (2.10) and should be the same in flat space as on the sphere. Unlike a mass term, with $\beta_{m^2} = \gamma_{\sigma^2} m^2$, the renormalization of η receives an additional contribution at leading order from the κ vertex in Figure 2.5 (b). However, [66, 67, 86, 87] all find at leading order that $\beta_\eta = \gamma_{\sigma^2}^{\text{irred.}} \eta$ and $\beta_{m^2} = \gamma_{\sigma^2}^{\text{irred.}} m^2$, where $\gamma_{\sigma^2}^{\text{irred.}}$ does not include reducible diagrams. The discrepancy in the g^4 term in β_η cannot be resolved by including or omitting the reducible diagram $\mathcal{G}_4^{(3)}$ in Figure 2.1 in the two-point function, because the singularity structure does not match (see (2.8)).

Renormalization of curvature terms in the background field method was also considered by [88–90], who found results agreeing with [67] for the pure curvature terms, but did not compute two-loop beta functions for the curvature couplings to scalars.

E Details of long-range model calculations

In this appendix, we include some details of the renormalized free energy calculations in Section 4.

E.1 Quartic model

Note that the beta function (4.9) implies that in (4.8)

$$\delta_\lambda = \frac{2(N+8)}{(4\pi)^{\frac{d}{2}} \Gamma(\frac{d}{2})} \frac{\lambda^2}{\varepsilon} + \frac{4(N+8)^2}{(4\pi)^d \Gamma(\frac{d}{2})^2} \frac{\lambda^3}{\varepsilon^2} + \frac{4(5N+22)}{(4\pi)^d \Gamma(\frac{d}{2})^2} \left(\gamma_E + 2\psi\left(\frac{d}{4}\right) - \psi\left(\frac{d}{2}\right) \right) \frac{\lambda^3}{\varepsilon} + \mathcal{O}(\lambda^4). \quad (\text{E.1})$$

The diagrams that contribute to (4.11) are shown in Figure 1 of [16]. In the long-range model, they are

$$\begin{aligned} H_2 &= 8N(N+2)C_{d,s}^4 I_2(d-\varepsilon), \\ H_3 &= 64N(N+2)C_{d,s}^6 I_3(2(d-\varepsilon)), \\ H_4 &= 32(4!)N(N+2)C_{d,s}^8 \left((N^2+6N+20)H_4^{(1)} + 8(N+2)H_4^{(2)} + 4(5N+22)H_4^{(3)} \right), \end{aligned} \quad (\text{E.2})$$

¹¹The curvature counterterm $\sigma \mathcal{R}^2$ was not included in [86, 87].

where the $H_4^{(k)}$ are diagrams that are evaluated with Mellin-Barnes integrals directly in various integer dimensions:

$$\begin{aligned}
H_4^{(1)} &= (2R)^{4\epsilon} \begin{cases} -20\pi^4 \left(\frac{1}{\epsilon^2} + \frac{2}{\epsilon} + 4 \right) + \mathcal{O}(\epsilon^1), & d = 2, \\ 2^5 5\pi^6 \left(\frac{1}{3\epsilon} + \frac{4}{9}(4 - 3 \log 2) \right) + \mathcal{O}(\epsilon^1), & d = 3, \end{cases} \\
H_4^{(2)} &= (2R)^{4\epsilon} \begin{cases} 4\pi^4, & d = 2, \\ \mathcal{O}(\epsilon^1), & d = 3, \end{cases} \\
H_4^{(3)} &= (2R)^{4\epsilon} \begin{cases} -2\pi^4 \left(\frac{5}{\epsilon^2} + \frac{2(5+3 \log 2)}{\epsilon} + 2 \log^2 2 + 12 \log 2 + 20 \right) + \mathcal{O}(\epsilon^1), & d = 2, \\ 2^3 \pi^6 \left(\frac{10}{3} + \frac{1}{9}(178 - 9\pi - 84 \log 2) \right) + \mathcal{O}(\epsilon^1), & d = 3. \end{cases}
\end{aligned} \tag{E.3}$$

Substituting these values and the renormalized λ using (E.1) into (4.11), we find (4.12) and (4.13).

E.2 Cubic model

The diagrams correcting the three-point vertex were considered in momentum-space in [23]. Here, we evaluate them in the long-range model. The one-loop corrections of the cubic vertices, including the counterterm terms, take the following form:

$$-(g_1 + \delta_{g_1}) - (g_1 + g_2)g_1^2 I, \quad -(g_2 + \delta_{g_2}) - (Ng_1^3 + g_2^3)I, \tag{E.4}$$

where I is the momentum space integral

$$I = \int \frac{d^d k}{(2\pi)^d} \frac{1}{|k|^s |p - k|^s |k + q|^s}. \tag{E.5}$$

Here we have used the momentum space representation $G(p) = \frac{1}{|p|^s}$ of the free propagator in the long-range model. We evaluate the integral I by using Feynman parameterization:

$$\begin{aligned}
I &= \int_0^1 \frac{dx dy dz}{xyz} \frac{\delta(1 - x - y - z)(xyz)^{\frac{s}{2}} \Gamma(\frac{3s-d}{2})}{(4\pi)^{\frac{d}{2}} \Gamma(\frac{s}{2})^3 \Delta^{\frac{3s-d}{2}}}, \\
\Delta &= x(1-x)p^2 + y(1-y)q^2 + 2xyp \cdot q.
\end{aligned} \tag{E.6}$$


Because $3s - d = 2\epsilon$, the integral I has a $1/\epsilon$ pole:

$$I = \frac{1}{(4\pi)^{\frac{d}{2}} \Gamma(\frac{d}{2}) \epsilon} + \mathcal{O}(\epsilon^0). \tag{E.7}$$

From this divergence, we can directly find the leading-order beta functions (4.16). The free energy (4.17) involves the diagrams

$$G_2 = 3!t_2 C_{d,s}^3 I_2(d - \varepsilon), \quad (\text{E.8})$$

$$G_4 = 3(3!)^3 C_{d,s}^6 (3t_{41} G_4^{(1)} + 2t_{42} G_4^{(2)}), \quad (\text{E.9})$$

where the t coefficients are given by (C.7). $G_4^{(1)}$ (corresponding to the diagram ) is of order ε in odd dimensions and is finite in even dimensions,¹² e.g.

$$G_4^{(1)} = (2R)^{4\varepsilon} \begin{cases} 9\pi^4 + \mathcal{O}(\varepsilon^1), & d = 2, \\ -\frac{27\pi^8}{80} + \mathcal{O}(\varepsilon^1), & d = 4. \end{cases} \quad (\text{E.10})$$

$G_4^{(2)}$ (corresponding to the diagram ) is finite in odd d , e.g.

$$G_4^{(2)} = (2R)^{4\varepsilon} \begin{cases} 4\pi^8 + \mathcal{O}(\varepsilon^1), & d = 3, \\ -\frac{9\pi^{12}}{10\Gamma(\frac{1}{3})^3} + \mathcal{O}(\varepsilon^1), & d = 5. \end{cases} \quad (\text{E.11})$$

and contains a $1/\varepsilon$ pole in even d , e.g.

$$G_4^{(2)} = (2R)^{4\varepsilon} \begin{cases} -\frac{3}{4}\pi^{5/2}\Gamma(\frac{1}{6})^3 \left(\frac{1}{\varepsilon} + 2\right) + \mathcal{O}(\varepsilon^1), & d = 2, \\ \frac{27\pi^{19/2}}{\Gamma(\frac{1}{6})^3} \left(\frac{1}{\varepsilon} + 3\right) + \mathcal{O}(\varepsilon^1), & d = 4. \end{cases} \quad (\text{E.12})$$

Then we have, including terms that will be of order ε^2 at the fixed point of (4.16), and using the definition (4.4),

$$\begin{aligned} \delta\tilde{F}^{\text{LR}} &= -\frac{1}{288\pi^2}(3Ng_1^2 + g_2^2)\varepsilon - \frac{1}{1152\pi^4}(3Ng_1^4 + 4Ng_1^3g_2 + g_2^4), & d = 3, \\ \frac{2}{\pi}\delta\tilde{F}^{\text{LR}} &= -\frac{\Gamma(\frac{7}{6})^3}{576\pi^{7/2}}(3Ng_1^2 + g_2^2)\varepsilon - \frac{\Gamma(\frac{7}{6})^3}{9216\pi^{11/2}}(3Ng_1^4 + 4Ng_1^3g_2 + g_2^4), & d = 4, \\ \delta\tilde{F}^{\text{LR}} &= -\frac{\Gamma(\frac{4}{3})^3}{90(4\pi)^3}(3Ng_1^2 + g_2^2)\varepsilon - \frac{4\Gamma(\frac{4}{3})^3}{135(4\pi)^6}(3Ng_1^4 + 4Ng_1^3g_2 + g_2^4), & d = 5. \end{aligned} \quad (\text{E.13})$$

For $N = -2$ at the fixed point, we have

$$\begin{aligned} \tilde{F}^{\text{LR}} &= -\tilde{F}_{\text{free}}^{\text{LR}} - \frac{\varepsilon^2}{432}, & d = 3, \\ a^{\text{LR}} &= -\frac{2}{\pi}\tilde{F}_{\text{free}}^{\text{LR}} - \frac{\Gamma(\frac{7}{6})^3}{216\pi^{3/2}}\varepsilon^2, & d = 4, \\ \tilde{F}^{\text{LR}} &= -\tilde{F}_{\text{free}}^{\text{LR}} - \frac{\Gamma(\frac{4}{3})^3}{1440}\varepsilon^2, & d = 5. \end{aligned} \quad (\text{E.14})$$

¹²The finiteness of this diagram is closely related to the non-renormalization property of ϕ and σ .

Bibliography

- [1] S. L. Adler, *Massless, Euclidean Quantum Electrodynamics on the Five-Dimensional Unit Hypersphere*, Phys. Rev. D **6** (1972) 3445–3461. [Erratum: Phys.Rev.D 7, 3821 (1973)].
- [2] G. W. Gibbons and S. W. Hawking, *Action Integrals and Partition Functions in Quantum Gravity*, Phys. Rev. D **15** (1977) 2752–2756.
- [3] J. L. Cardy, *Is There a c Theorem in Four-Dimensions?*, Phys. Lett. B **215** (1988) 749–752.
- [4] D. L. Jafferis, I. R. Klebanov, S. S. Pufu, and B. R. Safdi, *Towards the F -Theorem: $N=2$ Field Theories on the Three-Sphere*, JHEP **06** (2011) 102, [[arXiv:1103.1181](#)].
- [5] I. R. Klebanov, S. S. Pufu, and B. R. Safdi, *F -Theorem without Supersymmetry*, JHEP **10** (2011) 038, [[arXiv:1105.4598](#)].
- [6] A. B. Zamolodchikov, *Irreversibility of the Flux of the Renormalization Group in a 2D Field Theory*, JETP Lett. **43** (1986) 730–732.
- [7] I. Jack and H. Osborn, *Analogues for the c Theorem for Four-dimensional Renormalizable Field Theories*, Nucl. Phys. B **343** (1990) 647–688.
- [8] Z. Komargodski and A. Schwimmer, *On Renormalization Group Flows in Four Dimensions*, JHEP **12** (2011) 099, [[arXiv:1107.3987](#)].
- [9] R. C. Myers and A. Sinha, *Seeing a c -theorem with holography*, Phys. Rev. D **82** (2010) 046006, [[arXiv:1006.1263](#)].
- [10] H. Casini, M. Huerta, and R. C. Myers, *Towards a derivation of holographic entanglement entropy*, JHEP **05** (2011) 036, [[arXiv:1102.0440](#)].
- [11] H. Casini and M. Huerta, *On the RG running of the entanglement entropy of a circle*, Phys. Rev. D **85** (2012) 125016, [[arXiv:1202.5650](#)].
- [12] S. S. Pufu, *The F -Theorem and F -Maximization*, J. Phys. A **50** (2017), no. 44 443008, [[arXiv:1608.02960](#)].
- [13] I. R. Klebanov, S. S. Pufu, S. Sachdev, and B. R. Safdi, *Entanglement Entropy of 3-d Conformal Gauge Theories with Many Flavors*, JHEP **05** (2012) 036, [[arXiv:1112.5342](#)].
- [14] G. Tarnopolsky, *Large N expansion of the sphere free energy*, Phys. Rev. D **96** (2017), no. 2 025017, [[arXiv:1609.09113](#)].
- [15] S. Giombi and I. R. Klebanov, *Interpolating between a and F* , JHEP **03** (2015) 117, [[arXiv:1409.1937](#)].

- [16] L. Fei, S. Giombi, I. R. Klebanov, and G. Tarnopolsky, *Generalized F-Theorem and the ϵ Expansion*, JHEP **12** (2015) 155, [[arXiv:1507.01960](#)].
- [17] S. Giombi, I. R. Klebanov, and G. Tarnopolsky, *Conformal QED_d, F-Theorem and the ϵ Expansion*, J. Phys. A **49** (2016), no. 13 135403, [[arXiv:1508.06354](#)].
- [18] L. Fei, S. Giombi, I. R. Klebanov, and G. Tarnopolsky, *Yukawa CFTs and Emergent Supersymmetry*, PTEP **2016** (2016), no. 12 12C105, [[arXiv:1607.05316](#)].
- [19] W. Zhu, C. Han, E. Huffman, J. S. Hofmann, and Y.-C. He, *Uncovering Conformal Symmetry in the 3D Ising Transition: State-Operator Correspondence from a Quantum Fuzzy Sphere Regularization*, Phys. Rev. X **13** (2023), no. 2 021009, [[arXiv:2210.13482](#)].
- [20] M. Dedushenko, *Ising BCFT from Fuzzy Hemisphere*, [arXiv:2407.15948](#).
- [21] Z. Zhou and Y. Zou, *Studying the 3d Ising surface CFTs on the fuzzy sphere*, [arXiv:2407.15914](#).
- [22] L. Hu, W. Zhu, and Y.-C. He, *Entropic F-function of 3D Ising conformal field theory via the fuzzy sphere regularization*, [arXiv:2401.17362](#).
- [23] L. Fei, S. Giombi, and I. R. Klebanov, *Critical $O(N)$ models in $6 - \epsilon$ dimensions*, Phys. Rev. D **90** (2014), no. 2 025018, [[arXiv:1404.1094](#)].
- [24] L. Fei, S. Giombi, I. R. Klebanov, and G. Tarnopolsky, *Three loop analysis of the critical $O(N)$ models in $6 - \epsilon$ dimensions*, Phys. Rev. D **91** (2015), no. 4 045011, [[arXiv:1411.1099](#)].
- [25] J. A. Gracey, *Four loop renormalization of ϕ^3 theory in six dimensions*, Phys. Rev. D **92** (2015), no. 2 025012, [[arXiv:1506.03357](#)].
- [26] M. Borinsky, J. A. Gracey, M. V. Kompaniets, and O. Schnetz, *Five-loop renormalization of ϕ^3 theory with applications to the Lee-Yang edge singularity and percolation theory*, Phys. Rev. D **103** (2021), no. 11 116024, [[arXiv:2103.16224](#)].
- [27] I. R. Klebanov and G. Tarnopolsky, *Uncolored random tensors, melon diagrams, and the Sachdev-Ye-Kitaev models*, Phys. Rev. D **95** (2017), no. 4 046004, [[arXiv:1611.08915](#)].
- [28] S. Giombi, I. R. Klebanov, and G. Tarnopolsky, *Bosonic tensor models at large N and small ϵ* , Phys. Rev. D **96** (2017), no. 10 106014, [[arXiv:1707.03866](#)].
- [29] D. Benedetti, R. Gurau, and S. Harribey, *Line of fixed points in a bosonic tensor model*, JHEP **06** (2019) 053, [[arXiv:1903.03578](#)].

- [30] L. Fraser-Taliente and J. Wheeler, *F-extremization determines certain large- N CFTs*, [arXiv:2412.10499](#).
- [31] M. E. Fisher, *Yang-lee edge singularity and ϕ^3 field theory*, Phys. Rev. Lett. **40** (Jun, 1978) 1610–1613.
- [32] J. L. Cardy, *Conformal invariance and the yang-lee edge singularity in two dimensions*, Phys. Rev. Lett. **54** (Apr, 1985) 1354–1356.
- [33] I. R. Klebanov, V. Narovlansky, Z. Sun, and G. Tarnopolsky, *Ginzburg-Landau description and emergent supersymmetry of the (3, 8) minimal model*, JHEP **02** (2023) 066, [[arXiv:2211.07029](#)].
- [34] Y. Nakayama and T. Tanaka, *Infinitely many new renormalization group flows between Virasoro minimal models from non-invertible symmetries*, JHEP **11** (2024) 137, [[arXiv:2407.21353](#)].
- [35] A. Katsevich, I. R. Klebanov, and Z. Sun, *Ginzburg-Landau description of a class of non-unitary minimal models*, [arXiv:2410.11714](#).
- [36] O. Delouche, J. E. Miro, and J. Ingoldby, *Testing the RG-flow $M(3, 10) + \phi_{1,7} \rightarrow M(3, 8)$ with Hamiltonian Truncation*, [arXiv:2412.09295](#).
- [37] L. Fei, S. Giombi, I. R. Klebanov, and G. Tarnopolsky, *Critical $Sp(N)$ models in $6 - \epsilon$ dimensions and higher spin dS/CFT* , JHEP **09** (2015) 076, [[arXiv:1502.07271](#)].
- [38] I. R. Klebanov, *Critical Field Theories with $OSp(1|2M)$ Symmetry*, Phys. Rev. Lett. **128** (2022), no. 6 061601, [[arXiv:2111.12648](#)].
- [39] S. Caracciolo, J. L. Jacobsen, H. Saleur, A. D. Sokal, and A. Sportiello, *Fermionic field theory for trees and forests*, Phys. Rev. Lett. **93** (2004) 080601, [[cond-mat/0403271](#)].
- [40] Y. Deng, T. M. Garoni, and D. Sokal, *Ferromagnetic phase transition for the spanning-forest model ($q \rightarrow 0$ limit of the Potts model) in three or more dimensions*, Phys. Rev. Lett. **98** (2007) 030602, [[cond-mat/0610193](#)].
- [41] R. Bauerschmidt, N. Crawford, T. Helmuth, and A. Swan, *Random spanning forests and hyperbolic symmetry*, Commun. Math. Phys. **381** (2021), no. 3 1223–1261, [[arXiv:1912.04854](#)].
- [42] M. Czakon, *Automatized analytic continuation of Mellin-Barnes integrals*, Comput. Phys. Commun. **175** (2006) 559–571, [[hep-ph/0511200](#)].

- [43] A. V. Smirnov and V. A. Smirnov, *On the Resolution of Singularities of Multiple Mellin-Barnes Integrals*, Eur. Phys. J. C **62** (2009) 445–449, [[arXiv:0901.0386](#)].
- [44] V. A. Smirnov, *Analytic tools for Feynman integrals*, vol. 250. Springer, 2012.
- [45] A. V. Belitsky, A. V. Smirnov, and V. A. Smirnov, *MB tools reloaded*, Nucl. Phys. B **986** (2023) 116067, [[arXiv:2211.00009](#)].
- [46] S. Giombi, R. Huang, I. R. Klebanov, S. S. Pufu, and G. Tarnopolsky, *The $O(N)$ Model in $4 < d < 6$: Instantons and complex CFTs*, Phys. Rev. D **101** (2020), no. 4 045013, [[arXiv:1910.02462](#)].
- [47] G. Arias-Tamargo, D. Rodriguez-Gomez, and J. G. Russo, *On the UV completion of the $O(N)$ model in $6 - \epsilon$ dimensions: a stable large-charge sector*, JHEP **09** (2020) 064, [[arXiv:2003.13772](#)].
- [48] M. Kompaniets and A. Pikelner, *Critical exponents from five-loop scalar theory renormalization near six-dimensions*, Phys. Lett. B **817** (2021) 136331, [[arXiv:2101.10018](#)].
- [49] O. Antipin, J. Bersini, F. Sannino, Z.-W. Wang, and C. Zhang, *More on the cubic versus quartic interaction equivalence in the $O(N)$ model*, Phys. Rev. D **104** (2021) 085002, [[arXiv:2107.02528](#)].
- [50] I. Jack and D. R. T. Jones, *Scaling dimensions at large charge for cubic ϕ^3 theory in six dimensions*, Phys. Rev. D **105** (2022), no. 4 045021, [[arXiv:2112.01196](#)].
- [51] A. Macfarlane and G. Woo, *ϕ^3 theory in six dimensions and the renormalization group*, Nuclear Physics B **77** (1974), no. 1 91–108.
- [52] O. F. de Alcantara Bonfim, J. E. Kirkham, and A. J. McKane, *Critical Exponents to Order ϵ^3 for ϕ^3 Models of Critical Phenomena in $6 - \epsilon$ dimensions*, J. Phys. A **13** (1980) L247. [Erratum: J.Phys.A 13, 3785 (1980)].
- [53] O. F. de Alcantara Bonfim, J. E. Kirkham, and A. J. McKane, *Critical exponents for the percolation problem and the yang-lee edge singularity*, Journal of Physics A: Mathematical and General **14** (sep, 1981) 2391.
- [54] M. C. Barbosa, M. A. Gusmao, and W. K. Theumann, *Renormalization and Phase Transitions in Potts ϕ^3 Field Theory with Quadratic and Trilinear Symmetry Breaking*, Phys. Rev. B **34** (1986) 3165–3176.
- [55] P. Mati, *Vanishing beta function curves from the functional renormalization group*, Phys. Rev. D **91** (2015), no. 12 125038, [[arXiv:1501.00211](#)].

- [56] P. Mati, *Critical scaling in the large- N $O(N)$ model in higher dimensions and its possible connection to quantum gravity*, Phys. Rev. D **94** (2016), no. 6 065025, [[arXiv:1601.00450](#)].
- [57] A. Eichhorn, L. Janssen, and M. M. Scherer, *Critical $O(N)$ models above four dimensions: Small- N solutions and stability*, Phys. Rev. D **93** (2016), no. 12 125021, [[arXiv:1604.03561](#)].
- [58] K. Kamikado and T. Kanazawa, *Nonperturbative RG analysis of five-dimensional $O(N)$ models with cubic interactions*, [arXiv:1604.04830](#).
- [59] L. Zambelli and O. Zanusso, *Lee-Yang model from the functional renormalization group*, Phys. Rev. D **95** (2017), no. 8 085001, [[arXiv:1612.08739](#)].
- [60] S. M. Chester, S. S. Pufu, and R. Yacoby, *Bootstrapping $O(N)$ vector models in $4 < d < 6$* , Phys. Rev. D **91** (2015), no. 8 086014, [[arXiv:1412.7746](#)].
- [61] Z. Li and N. Su, *Bootstrapping Mixed Correlators in the Five Dimensional Critical $O(N)$ Models*, JHEP **04** (2017) 098, [[arXiv:1607.07077](#)].
- [62] G. 't Hooft and M. J. G. Veltman, *Regularization and Renormalization of Gauge Fields*, Nucl. Phys. B **44** (1972) 189–213.
- [63] G. 't Hooft, *Dimensional regularization and the renormalization group*, Nuclear Physics **61** (1973) 455–468.
- [64] L. S. Brown and J. C. Collins, *Dimensional Renormalization of Scalar Field Theory in Curved Space-time*, Annals Phys. **130** (1980) 215.
- [65] S. J. Hathrell, *Trace Anomalies and $\lambda\phi^4$ Theory in Curved Space*, Annals Phys. **139** (1982) 136.
- [66] D. J. Toms, *Renormalization of Interacting Scalar Field Theories in Curved Space-time*, Phys. Rev. D **26** (1982) 2713.
- [67] I. Jack, *Renormalizability of ϕ^3 theory in 6-dimensional curved spacetime*, Nuclear Physics B **274** (1986), no. 1 139–156.
- [68] M. E. Fisher, S.-k. Ma, and B. G. Nickel, *Critical exponents for long-range interactions*, Phys. Rev. Lett. **29** (Oct, 1972) 917–920.
- [69] J. Sak, *Recursion Relations and Fixed Points for Ferromagnets with Long-Range Interactions*, Phys. Rev. B **8** (1973), no. 1 281.
- [70] J. Sak, *Low-temperature renormalization group for ferromagnets with long-range interactions*, Phys. Rev. B **15** (May, 1977) 4344–4347.

- [71] M. F. Paulos, S. Rychkov, B. C. van Rees, and B. Zan, *Conformal Invariance in the Long-Range Ising Model*, Nucl. Phys. B **902** (2016) 246–291, [[arXiv:1509.00008](#)].
- [72] C. Behan, L. Rastelli, S. Rychkov, and B. Zan, *Long-range critical exponents near the short-range crossover*, Phys. Rev. Lett. **118** (2017), no. 24 241601, [[arXiv:1703.03430](#)].
- [73] C. Behan, L. Rastelli, S. Rychkov, and B. Zan, *A scaling theory for the long-range to short-range crossover and an infrared duality*, J. Phys. A **50** (2017), no. 35 354002, [[arXiv:1703.05325](#)].
- [74] S. Giombi and H. Khanchandani, *$O(N)$ models with boundary interactions and their long range generalizations*, JHEP **08** (2020), no. 08 010, [[arXiv:1912.08169](#)].
- [75] D. Benedetti, R. Gurau, S. Harribey, and K. Suzuki, *Long-range multi-scalar models at three loops*, J. Phys. A **53** (2020), no. 44 445008, [[arXiv:2007.04603](#)].
- [76] D. Benedetti, R. Gurau, and S. Harribey, *Corrigendum and addendum: Long-range multi-scalar models at three loops*, [arXiv:2411.00805](#).
- [77] S. S. Gubser, C. Jepsen, S. Parikh, and B. Trundy, *$O(N)$ and $O(N)$ and $O(N)$* , JHEP **11** (2017) 107, [[arXiv:1703.04202](#)].
- [78] S. Giombi, E. Helfenberger, and H. Khanchandani, *Long range, large charge, large N* , JHEP **01** (2023) 166, [[arXiv:2205.00500](#)].
- [79] S. S. Gubser and I. R. Klebanov, *A Universal result on central charges in the presence of double trace deformations*, Nucl. Phys. B **656** (2003) 23–36, [[hep-th/0212138](#)].
- [80] D. E. Diaz and H. Dorn, *Partition functions and double-trace deformations in AdS/CFT*, JHEP **05** (2007) 046, [[hep-th/0702163](#)].
- [81] S. Giombi, I. R. Klebanov, S. S. Pufu, B. R. Safdi, and G. Tarnopolsky, *AdS Description of Induced Higher-Spin Gauge Theory*, JHEP **10** (2013) 016, [[arXiv:1306.5242](#)].
- [82] Z. Sun, *AdS one-loop partition functions from bulk and edge characters*, JHEP **12** (2021) 064, [[arXiv:2010.15826](#)].
- [83] L. Fraser-Taliente, C. P. Herzog, and A. Shrestha, *A Nonlocal Schwinger Model*, [arXiv:2412.02514](#).
- [84] J. Henriksson, *The critical $O(N)$ CFT: Methods and conformal data*, Phys. Rept. **1002** (2023) 1–72, [[arXiv:2201.09520](#)].

- [85] B. Nienhuis, *Exact critical point and critical exponents of $O(n)$ models in two-dimensions*, Phys. Rev. Lett. **49** (1982) 1062.
- [86] J. Kodaira and J. Okada, *Renormalizing $(\varphi^3)_6$ theory in curved space-time*, Phys. Rev. D **33** (May, 1986) 2875–2881.
- [87] J. Kodaira, *Interacting scalar field theory in general curved space-time*, Phys. Rev. D **33** (May, 1986) 2882–2892.
- [88] B. Grinstein, A. Stergiou, D. Stone, and M. Zhong, *Two-loop renormalization of multiflavor ϕ^3 theory in six dimensions and the trace anomaly*, Phys. Rev. D **92** (2015), no. 4 045013, [[arXiv:1504.05959](#)].
- [89] H. Osborn and A. Stergiou, *Structures on the Conformal Manifold in Six Dimensional Theories*, JHEP **04** (2015) 157, [[arXiv:1501.01308](#)].
- [90] A. Stergiou, D. Stone, and L. G. Vitale, *Constraints on Perturbative RG Flows in Six Dimensions*, JHEP **08** (2016) 010, [[arXiv:1604.01782](#)].
- [91] J. Cardy, *The Yang-Lee Edge Singularity and Related Problems*, 5, 2023. [[arXiv:2305.13288](#)].
- [92] F. Gliozzi and A. Rago, *Critical exponents of the 3d Ising and related models from Conformal Bootstrap*, JHEP **10** (2014) 042, [[arXiv:1403.6003](#)].
- [93] H. Kausch, G. Takacs, and G. Watts, *On the relation between $\Phi_{(1,2)}$ and $\Phi_{(1,5)}$ perturbed minimal models*, Nucl. Phys. B **489** (1997) 557–579, [[hep-th/9605104](#)].
- [94] T. Quella, I. Runkel, and G. M. T. Watts, *Reflection and transmission for conformal defects*, JHEP **04** (2007) 095, [[hep-th/0611296](#)].
- [95] E. Ardonne, J. Gukelberger, A. W. W. Ludwig, S. Trebst, and M. Troyer, *Microscopic models of interacting yang-lee anyons*, New Journal of Physics **13** (Apr., 2011) 045006, [[arXiv:1012.1080](#)].
- [96] I. T. Drummond, *Conformally Invariant Amplitudes and Field Theory in a Space-Time of Constant Curvature*, Phys. Rev. D **19** (1979) 1123.
- [97] I. T. Drummond, *Dimensional Regularization of Massless Theories in Spherical Space-Time*, Nucl. Phys. B **94** (1975) 115–144.